Developmental Biology 343 (2010) 1–17

Contents lists available at ScienceDirect

Developmental Biology

journal homepage: www.elsevier.com/developmentalbiology

Proneural gene-linked neurogenesis in zebrafish cerebellum

Shuichi Kani [a], Young-Ki Bae [a,b], Takashi Shimizu [a,c], Koji Tanabe [a], Chie Satou [d], Michael J. Parsons [e], Ethan Scott [f], Shin-ichi Higashijima [d], Masahiko Hibi [a,c,*]

[a] Laboratory for Vertebrate Axis Formation, RIKEN Center for Developmental Biology, Kobe, Hyogo, Japan
[b] Division of Basic and Applied Sciences, Research Institute, National Cancer Center, Republic of Korea
[c] Bioscience and Biotechnology Center, Nagoya University, Nagoya, Aichi, Japan
[d] National Institutes of Natural Sciences, Okazaki Institute for Integrative Bioscience, National Institute for Physiological Sciences, Okazaki, Aichi, Japan
[e] Department of Surgery, Johns Hopkins University, Baltimore, MD, USA
[f] The University of Queensland, School of Biomedical Science, St. Lucia 4072, Australia

ARTICLE INFO

Article history:
Received for publication 16 January 2010
Revised 30 March 2010
Accepted 31 March 2010
Available online 11 April 2010

Keywords:
Zebrafish
Cerebellum
Hindbrain
Glutamatergic neuron
GABAergic neuron
Proneural gene
Adult neurogenesis

ABSTRACT

In mammals, cerebellar neurons are categorized as glutamatergic or GABAergic, and are derived from progenitors that express the proneural genes *atoh1* or *ptf1a*, respectively. In zebrafish, three *atoh1* genes, *atoh1a*, *atoh1b,* and *atoh1c*, are expressed in overlapping but distinct expression domains in the upper rhombic lip (URL): *ptf1a* is expressed exclusively in the ventricular zone (VZ). Using transgenic lines expressing fluorescent proteins under the control of the regulatory elements of *atoh1a* and *ptf1a*, we traced the lineages of the cerebellar neurons. The *atoh1*$^+$ progenitors gave rise not only to granule cells but also to neurons of the anteroventral rhombencephalon. The *ptf1a*$^+$ progenitors generated Purkinje cells. The *olig2*$^+$ eurydendroid cells, which are glutamatergic, were derived mostly from *ptf1a*$^+$ progenitors in the VZ but some originated from the *atoh1*$^+$ progenitors in the URL. In the adult cerebellum, *atoh1a, atoh1b,* and *atoh1c* are expressed in the molecular layer of the valvula cerebelli and of the medial corpus cerebelli, and *ptf1a* was detected in the VZ. The proneural gene expression patterns coincided with the sites of proliferating neuronal progenitors in the adult cerebellum. Our data indicate that proneural gene-linked neurogenesis is evolutionarily conserved in the cerebellum among vertebrates, and that the continuously generated neurons help remodel neural circuits in the adult zebrafish cerebellum.

© 2010 Elsevier Inc. All rights reserved.

Introduction

The cerebellum forms in the dorsal anterior hindbrain and plays an important role in the integration of sensory perception and motor control. In mammals, it is involved in higher cognitive and emotional functions (Ito, 2002a,b, 2006, 2008), which requires the formation of neural circuits within the cerebellum and the connection of cerebellar neurons with the extracerebellar central nervous system. In zebrafish, as in mammals, the cerebellum contains several different types of neurons that are categorized into two groups according to their major neurotransmitter as glutamatergic or GABAergic (Altman and Bayer, 1997; Bae et al., 2009; Butler and Hodos, 1996). The glutamatergic neurons include the granule cells, unipolar brush cells, and eurydendroid cells; the latter are equivalent to the neurons in the mammalian deep cerebellar nuclei. The GABAergic neurons include Purkinje cells and interneurons such as the Golgi and stellate cells.

In the adult zebrafish, the cerebellar neurons and the neural fibers are arranged in a three-layer structure (from superficial to deep): the molecular layer, Purkinje cell layer, and granule cell layer. They are also arranged in three lobular structures, from rostral to caudal: the valvula cerebelli (Va), the corpus cerebelli (CCe), and the vestibulolateral lobe, which consists of the eminentia granularis (EG) and the lobus caudalis cerebelli (LCa) (Bae et al., 2009; Miyamura and Nakayasu, 2001; Wullimann et al., 1996). The Va, the CCe, and the lobus caudalis cerebelli have the same three-layer structure, whereas the eminentia granularis contains the only the granule cell layer. We previously reported that the differentiation of GABAergic and glutamatergic neurons begins at 3 days post-fertilization (dpf), and the layered and lobular structures are first detectable at 5 dpf during zebrafish development (Bae et al., 2009).

In the mouse, genetic studies show that the glutamatergic neurons are derived from progenitors located in the upper rhombic lip (URL) and express the proneural gene *Atoh1* (*Atonal homolog 1*, *Math1* in mice) (Alder et al., 1996; Ben-Arie et al., 1997). *Atoh1*-expressing URL progenitors sequentially generate neurons of the tegmental nuclei, the deep cerebellar nuclei, and the granule cells (Machold and Fishell, 2005; Wang et al., 2005; Wilson and Wingate, 2006; Wingate, 2005). The granule cell precursors from the URL initially expand in the germinal zone above the Purkinje cell layer, called the external granule cell layer (EGL), and then migrate below the Purkinje cell

* Corresponding author. Bioscience and Biotechnology Center, Nagoya University, Furocho, Chikusaku, Nagoya, 464-8601, Japan. Fax: +81 52 789 5053.
E-mail address: hibi@bio.nagoya-u.ac.jp (M. Hibi).

0012-1606/$ – see front matter © 2010 Elsevier Inc. All rights reserved.
doi:10.1016/j.ydbio.2010.03.024

layer to form the granule cell layer (also called the IGL) (Altman and Bayer, 1997). The granule cells express another proneural gene *NeuroD*, which is required for generation of the granule cells (Miyata et al., 1999). The GABAergic neurons of the mouse cerebellum are derived from progenitors in the VZ that express the proneural gene *Ptf1a* (Hoshino, 2006; Hoshino et al., 2005).

In the zebrafish cerebellum, the *atoh1* genes *atoh1a* and *atoh1b* are expressed in the URL (Adolf et al., 2004; Köster and Fraser, 2001); *ptf1a* is expressed in the VZ (Elsen et al., 2009; Lin et al., 2004; Volkmann et al., 2008; Zecchin et al., 2004), like its orthologue in the mouse. The descendents of the URL-based progenitors migrate rostrally and then ventrally to settle outside the cerebellum in zebrafish (Köster and Fraser, 2001), as the descendants of *Atoh1*$^+$ cells migrate to the pontomesencephalic tegmentum (Machold and Fishell, 2005; Wang et al., 2005). Furthermore, studies with a transgenic zebrafish line expressing GFP in the granule cell lineage revealed that the URL-derived cells migrate along different paths to generate the granule cells in the CCe, eminentia granularis, and lobus caudalis cerebelli (Köster and Fraser, 2006; Rieger et al., 2009; Volkmann et al., 2008). It is reported that cell proliferation takes place in the cerebellar region, including the external granule cell layer, where *neurod* is expressed, between 2 and 5 dpf; the postmitotic granule cells are derived from the proliferating zones (Mueller and Wullimann, 2002; Wullimann and Knipp, 2000). These data suggest that the zebrafish and mouse cerebellum use similar mechanisms to control cerebellar neurogenesis. However, it has recently been reported that zebrafish and shark cerebellums do not have a typical external granule germinal layer, which is a zone for transit amplification of the granule cells (Chaplin et al., 2010). Therefore it is not yet clear how the *atoh1*-expressing progenitors produce the granule cells and other populations in the zebrafish cerebellum. Furthermore, whether the *ptf1a*-expressing progenitors generate GABAergic neurons, such as Purkinje cells, in the zebrafish cerebellum is not reported.

In addition to the *atoh1* and *ptf1a* genes, the proneural gene *olig2* is expressed in the cells which are located in the vicinity of the Purkinje cells (Bae et al., 2009; McFarland et al., 2008). Marker analysis with a *Tg(olig2:EGFP)* line reveal that the majority of *olig2*-expressing cells are large cells and stained with a neuronal marker but not with oligodendrocyte markers (Bae et al., 2009). Retrograde labeling analysis shows that at least some *olig2*-expressing cells send their axons to the pretectal region, where many eurydendroid cells send their axons (Bae et al., 2009). These data indicate that, although *olig2*$^+$ cells include oligodendrocytes, the majority of them are eurydendroid cells. *olig2* is also expressed in the VZ of adult zebrafish cerebellum (Bae et al., 2009), suggesting that *olig2*$^+$ eurydendroid cells are derived from the VZ-based progenitors. Although *Ptf1a*$^+$ progenitors in the VZ generate the GABAergic neurons in the mouse cerebellum, the *olig2*$^+$ eurydendroid cells are glutamatergic (Bae et al., 2009). Thus, it is not clear if the GABAergic neurons and the *olig2*$^+$ eurydendroid cells are derived from the same progenitors in the VZ.

In the adult mammalian central nervous system, there are only a few restricted domains that exhibit neurogenesis, such as the dentate gyrus of the hippocampus (Altman and Das, 1965; Gould et al., 1998) and the subventricular zone of the ventral forebrain, which produces olfactory bulb interneurons (Altman, 1969; Eriksson et al., 1998; Lois and Alvarez-Buylla, 1994; Luskin, 1993). The central nervous system of teleost species has dozens of proliferation zones that generate new neurons (Adolf et al., 2006; Ekström et al., 2001; Grandel et al., 2006; Zikopoulos et al., 2000; Zupanc et al., 2005; Zupanc and Horschke, 1995). In the zebrafish adult cerebellum, BrdU incorporation and proliferation marker analyses show that proliferating progenitors are located in the molecular layer of the Va and of the medial region of the CCe (Grandel et al., 2006; Kaslin et al., 2009; Zupanc et al., 2005). These proliferating cells are positive for Nestin, which is also expressed in mammalian neural stem cells (Kaslin et al., 2009); they do not express *atoh1a, atoh1b, ptf1a*, or radial glial markers (Kaslin et al., 2009). It remains to be elucidated whether these proliferating cells are a unique population or if they include various types of neuronal progenitors and neural stem cells.

In this study, we first examined the expression of the proneural genes *atoh1a, atoh1b, atoh1c*, and *ptf1a*. Then, we carried out lineage tracing of the cerebellar neurons using transgenic zebrafish lines expressing fluorescent proteins driven by regulatory elements of the proneural genes. We demonstrate that the process that generates glutamatergic and GABAergic neurons from progenitors in the URL and VZ is conserved between mammals and zebrafish. Furthermore, we found that *olig2*$^+$ eurydendroid cells are derived from both *ptf1a*$^+$ and *atoh1a*$^+$ progenitors. Unlike in the mammalian cerebellum, the *atoh1* genes and *ptf1a* are also expressed in the adult cerebellum and mark adult neuronal progenitors. Our findings demonstrate that the zebrafish cerebellum is a good model system for studying neurogenesis, remodeling of the neural system, and their abnormalities in the vertebrate cerebellum.

Materials and methods

Zebrafish wild-type and transgenic lines

Wild-type zebrafish (*Danio rerio*) with the Oregon AB genetic background were used. Transgenic lines *Tg(olig2:EGFP)vu12* (Shin et al., 2003), *Tg(ptf1a:EGFP)jh1* (Pisharath et al., 2007), *Tg(vglut2a:EGFP)* (Bae et al., 2009), *Tg(UAS-E1b:NfsB-mCherry)c264* (Davison et al., 2007) were previously reported. *Et(fos:Gal4-VP16)s1168t/+; Tg(UAS-E1b: Kaede)s1999t/+* was isolated in a GAL4 enhancer trap screen (Scott and Baier, 2009; Scott et al., 2007). *Tg(atoh1a:EGFP), Tg(atoh1a:dTomato)*, and *Tg(vglut2a:DsRed2)* were constructed using the BAC CHORI211-247L22 and DEKY-145P2, by a previously described method (Kimura et al., 2006). The details for generating these lines and *Tg(ptf1a:Gal4-VP16)* will be described elsewhere.

Zebrafish were reared as described (Westerfield, 1995). For immunohistochemistry and whole-mount in situ hybridization, embryos and larvae were treated with 0.005% phenylthiourea from 12 hpf to prevent the development of pigmentation. Developmental stages were determined according to the Zebrafish Information Network (ZFIN: http://zfin.org/). Embryos are defined as <3 days old; larvae are between 3 and 29 days old; juvenile fish are between 30 and 89 days old; adult fish are 90 days old or older.

In situ hybridization

The *atoh1a* cDNA was previously reported (Kim et al., 1997). The *atoh1b* (Adolf et al., 2004) and *ptf1a* (Lin et al., 2004; Zecchin et al., 2004) cDNAs were obtained by reverse-transcription PCR from zebrafish embryos and were used to generate riboprobes. A fragment of the *atoh1c* gene was initially identified by searching for *atoh1a* homologous genes with the Ensemble genome browser (http://uswest.ensembl.org/Danio_rerio/). The full-length *atoh1c* cDNA was isolated by 5'- and 3'-RACE (rapid amplification of cDNA ends) method, using a SMART RACE cDNA amplification kit (Takara-Clontech). The sequence information of *atoh1c* was deposited under accession number AB530457 in the DDBJ databank. The *atoh1c* gene was also reported recently (Chaplin et al., 2010; Wang et al., 2009). Detailed information about these probes is available on request.

Whole-mount in situ hybridization was performed as described previously (Thisse and Thisse, 1998) except hybridization was at 65 °C. Plastic sections were made from stained embryos or larvae using Technovit 8100 (Heraeus Kulzer). For sectioning, embryos and larvae were fixed overnight at 4 °C in 4% paraformaldehyde (PFA) in phosphate-buffered saline (PBS). The specimens were immersed in 30% sucrose solution overnight at 4 °C, frozen in OCT compound (Sakura Finetechnical), and sectioned at 12–14 μm on a cryostat. The in situ hybridization of the sections was carried out as described

previously (Bae et al., 2009). For the single-color observation of section and whole-mount in situ hybridization, NBT/BCIP (Roche) was used as the substrate for alkaline phosphatase. For two-color fluorescence in situ hybridization, tyramide signal amplification (TSA) kits with the Cy3 and FITC fluorphores (PerkinElmer) were used. The NBT/BCIP signals were acquired using an AxioPlan-2 microscope and AxioCam CCD camera (Zeiss). The fluorescence images were obtained as described below (under Immunohistochemistry).

Generation of anti-Neurod antibody

To raise monoclonal antibodies against Neurod, glutathione S-transferase (GST) fusion proteins containing amino acids 1–57 of Neurod were generated in *Escherichia coli* BL21DE3. The GST fusion proteins were purified by Glutathione Sepharose 4B (GE Healthcare) and used for immunization. Balb/c mice were immunized four times with about 50 μg of the proteins. Spleen cells of the immunized mice were fused with the mouse myeloma line Ag8.563, and hybridomas were obtained by conventional HAT selection. The supernatants of growth-positive cells were tested in enzyme-linked immunosorbent assays (ELISAs) to identify hybridoma clones producing specific antibodies.

Immunohistochemistry

For immunostaining, anti-GFP (1/1000, mouse or rabbit, Nacalai), anti-HuC/D (1/500, mouse, Molecular Probes, Invitrogen), anti-Kaede (1/1000, rabbit, MBL Co. Ltd.), anti-DsRed (mCherry, 1/1000, rabbit, Takara-Clontech), anti-BrdU (1/1000, BD Bioscience), anti-parvalbumin 7 (1/1000, mouse ascites) (Bae et al., 2009), and anti-Neurod (1/500, mouse ascites) antibodies were used. Immunostaining of embryos and larvae or of the cryosections was performed as described previously (Bae et al., 2009). Alexa Fluor 488 and/or Alexa Fluor 555 goat anti-mouse and/or goat anti-rabbit IgG (H+L, Molecular Probes, Invitrogen) were used as secondary antibodies. For two-color staining with two mouse monoclonal antibodies, a Zenon antibody labeling kit (Molecular Probes, Invitrogen) was used. The Vectastain Elite ABC kit (Vector) was also used for immunostaining with the horseradish peroxidase (HRP) substrate diaminobenzidine (DAB). When the samples were stained with a riboprobe and antibody, in situ hybridization (NBT/BCIP or TSA staining) was performed first, followed by immunostaining (DAB or fluorescence). The fluorescent images and DAB signals were obtained with a LSM5 Pascal laser-scanning inverted microscope and AxioPlan-2 microscope, respectively. The fluorescent images were constructed from Z-stack sections by a 3D projection program associated with the microscope. Figures were constructed using Adobe Photoshop. Alexa Fluor 488 and FITC signals were colored green; Alex 555 and Cy3 signals were colored magenta, for the figures.

BrdU incorporation

Larvae or adult fish were kept in 1% BrdU (5'-bromo-deoxyuridine, Wako) solution for 1 h in the dark. For the birthdate analysis, the larvae or fish were then moved to be kept in the BrdU-free water for 3 to 5 days. The larvae or the brains were fixed in 4% PFA in PBS. The larvae or the cryosections of the brains were treated with 2N HCl for 30 min at room temperature, washed twice with PBS, 0.1% Tween20, neutralized twice with 0.1 M $Na_2B_4O_7$, and washed twice with PBS, 0.1% Tween20. Immunostaining was carried out as described above.

Cell tracing with Kaede

The rostral cerebellum of the transgenic fish expressing Kaede was irradiated with ultra violet (UV) light using a UV filter and diaphragm fitted on an AxioPlan-2. The green and red Kaede signals were obtained by the LSM5 Pascal laser-scanning inverted microscope.

Results

Expression of proneural genes in the zebrafish larval cerebellum

We first examined the expression patterns of the *atoh1* genes and *ptf1a*, the orthologues of which mark glutamatergic and GABAergic neuronal progenitors, respectively, in the mammalian cerebellum, and compared their expression domains during cerebellar development (Fig. 1). Two zebrafish *atoh1* genes, *atoh1a* (also called *zath1, atoh1.1*) and *atoh1b* (*zath1b, atoh1.2*) were previously reported (Adolf et al., 2004; Kim et al., 1997). In this study, by searching the annotated database provided by the zebrafish genome project (see Experimental Procedures), we also found a partial cDNA fragment of another *atoh1* paralogue, *atoh1c*. We isolated its full-length cDNA by the rapid amplification of cDNA ends (RACE).

During the pharyngula period (1 and 2 dpf), both *atoh1a* and *atoh1b* were expressed in the URL and lower rhombic lip (LRL) (Fig. 1A, B, F, G), as reported previously (Adolf et al., 2004; Bae et al., 2005; Köster and Fraser, 2001). At these stages, whereas *atoh1a* mRNA was broadly detected in the URL and LRL (Fig. 1A, B), *atoh1b* mRNA was enriched in the rostral half of the URL and the ventral part of the LRL (Fig. 1F, G). *atoh1c* was first detected at 2 dpf in the caudal URL but not in the LRL (Fig. 1K). In the early larval stages (2.5–5 dpf), the *atoh1a* transcripts were confined to the rostro-medial cerebellum (Fig. 1C–E), which corresponds to the Va. *atoh1b* is strongly expressed in the Va and weakly at the midline of the CCe and in the EG and the LCa (Fig. 1H–J). *atoh1c* is expressed in the midline of the CCe and in the EG and the LCa, but not in the Va (Fig. 1L–N). Thus, the *atoh1* genes were expressed in overlapping but distinct domains in the glutamatergic progenitors of the URL, similar to the URL-restricted expression of *Atoh1* in the mouse.

Consistent with previous reports (Elsen et al., 2009; Lin et al., 2004; Volkmann et al., 2008; Zecchin et al., 2004), *ptf1a* was first detected in the cerebellar primordium at 2 dpf (Fig. 1P) and was expressed throughout the early larval stages (Fig. 1Q–S). Sagittal and transverse sections (Fig. 1Ba–c, Pa–c) revealed that *atoh1a* transcripts were strictly localized to the dorsal surface, which corresponds to the URL; *ptf1a* was detected in the deep domains abutting either the fourth ventricle or cerebral aqueduct (Ca in Fig. 1Bb, Pb), corresponding to the VZ, at 2 dpf. Two-color in situ hybridization (Fig. 1T–W) confirmed the *atoh1a* expression in the Va and rostral CCe and the *ptf1a* expression in the VZ of the CCe, and showed that the *atoh1a* and *ptf1a* expression domains never overlapped at the stages examined (3 and 5 dpf). Thus, the expression of *atoh1* genes in the URL and of *ptf1a* in the VZ is conserved between zebrafish and mammals. The expression of *atoh1a, b, c*, and *ptf1a* in the embryonic and early larval stages is summarized in Fig. 1X.

Development of atoh1a-positive lineage

In an attempt to trace neuronal lineages in the zebrafish cerebellum, we used transgenic lines that express the genes for fluorescent proteins under the control of enhancer and promoter elements of the proneural genes. To this end, we used a strategy of BAC (bacterial artificial chromosome) homologous recombination (Lee et al., 2001) and transgenic technology (Kimura et al., 2006) to generate the transgenic fish. The fluorescent proteins we chose, EGFP and mCherry, are stable and can be detected for long periods after their translation. Therefore, we were able to monitor the neuronal progenitors expressing a given proneural gene and some of their progenies.

First, we verified the expression patterns of the fluorescent proteins. At 2 dpf, we found that the expression domains of *atoh1a* mRNA and EGFP in *Tg(atoh1a:EGFP)* almost completely overlapped in the cerebellum (Fig. 2A), indicating that the EGFP expression in the transgenic line (atoh1a:EGFP) recapitulates the endogenous *atoh1a* expression at the beginning of its expression. Next, we followed the

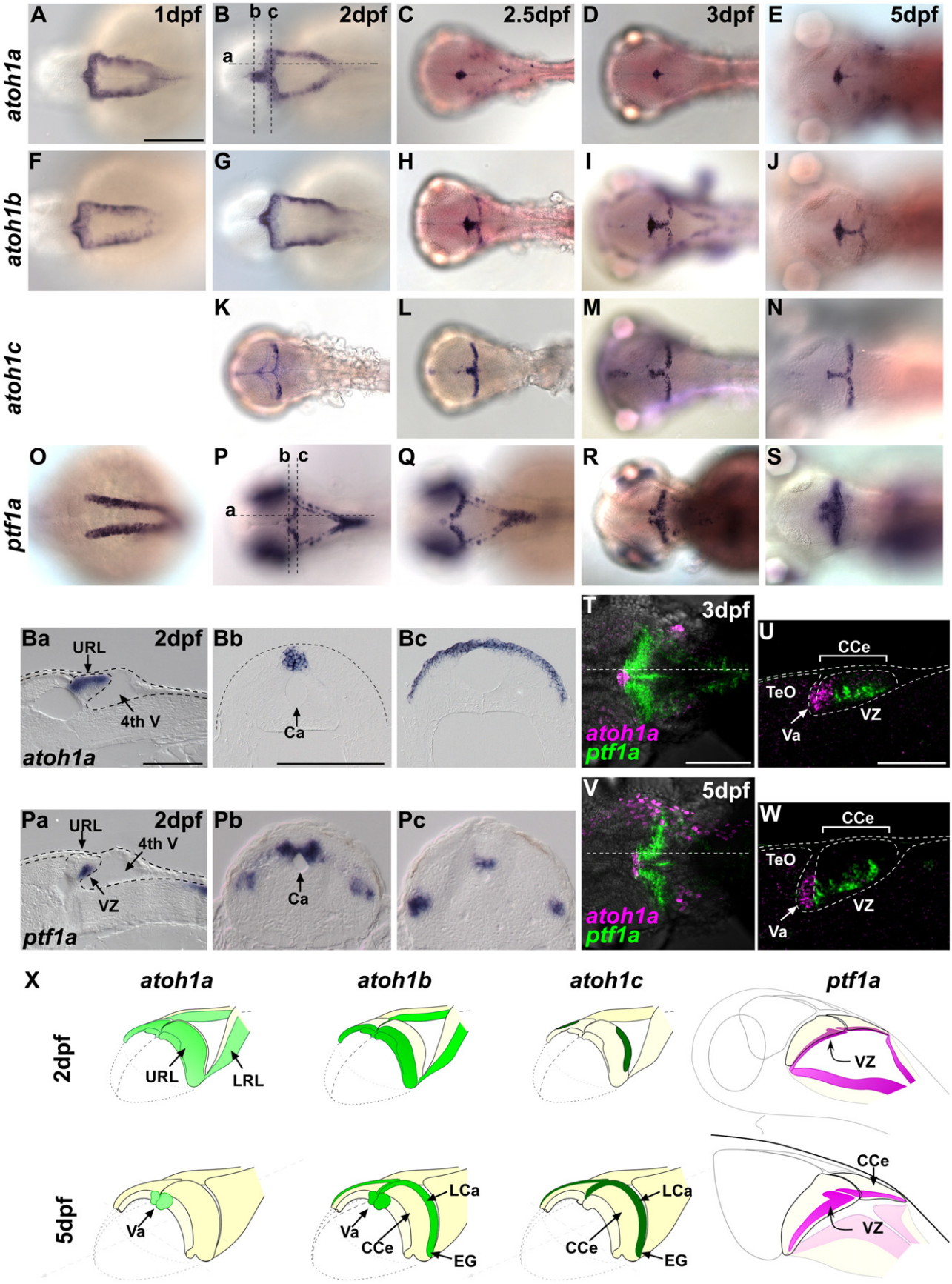

Fig. 1. Expression of proneural genes during cerebellar development. (A–S) Expression of *atoh1a* (A–E), *atoh1b* (F–J), *atoh1c* (K–N), and *ptf1a* (O–S) at dpf 1 (A, F, O), 2 (B, G, K, P), 2.5 (C, H, L, Q), 3 (D, I, M, R), and 5 (E, J, N, S). Dorsal views with rostral to the left. (Ba–c, Pa–c) Parasagittal (a) and cross sections (b, c) at the levels indicated in (B) and (P). (T–W) Co-staining of *atoh1a* and *ptf1a* expression at 3 (T, U) and 5 dpf (V, W). Dorsal views (T, V) and sagittal sections (U, W) at the levels indicated in (T) and (V). (X) Schematic representation of expression of *atoh1a* (light green), *atoh1b* (green), *atoh1c* (dark green), and *ptf1a* (pink) at 2 and 5 dpf. Ca, cerebral aqueduct; CCe, corpus cerebelli; EG, eminentia granularis; LCa, lobus caudalis cerebelli; LRL, lower rhombic lip; TeO, tectum opticum; URL, upper rhombic lip; Va, valvula cerebelli; VZ, ventricular zone; 4th V, fourth ventricle. Scale bars: 200 μm (A, T), 100 μm (Ba, Bb, U).

progeny of the *atoh1a*-expressing cells. During the early larval stages (3 and 5 dpf), atoh1a:EGFP was detected in not only the *atoh1a*-expressing cells in the Va but also the *atoh1a*-non-expressing cells of the CCe (Fig. 2B, C), indicating that the atoh1a:EGFP$^+$ cells included progenies of the *atoh1a*$^+$ neuronal progenitors. In the LRL at 1 dpf, the atoh1a:EGFP$^+$ cells migrated ventrally (Fig. 2G, Suppl. Movie 1), and these cells likely contributed to precerebellar nuclei, as reported for mouse hindbrain (Machold and Fishell, 2005; Wang et al., 2005).

In the URL, most atoh1a:EGFP$^+$ cells migrated rostrally from 1 to 2 dpf, and some of them gave rise to the Va, which is located at the rostral tip of the cerebellum, at 2 dpf (Fig. 2B, D, E, G, H, Suppl. Movie 1). During this period, a portion of the atoh1a:EGFP$^+$ cells migrated ventrally and eventually exited the cerebellum to form nuclei in the tegmentum on both sides of the cerebellum (Fig. 2H, M). These cells projected their axons to either the optic tectum (arrowheads, Fig. 2H, I, K, L) or hypothalamus (arrows, Fig. 2H, I, K, L). Although these cells did not express endogenous *atoh1a*, they continuously expressed EGFP in the adult cerebellum (Suppl. Fig. 1). A comparison of this cell population with the atlas of zebrafish brain (Wullimann et al., 1996) suggests that these tegmental nuclei include the secondary gustatory nuclei (SGN).

We further tried to confirm this migration to the anteroventral rhombencephalon (tegmentum) by lineage tracing using Gal4 enhancer trap lines and the photo-convertible Kaede protein. *Et(fos:Gal4-VP16)s1168t*:*Tg(UAS-E1b:Kaede)s1999t* (Gal4^{s1168t}; UAS-Kaede in Fig. 2) was isolated by an enhancer trap screen (Scott and Baier, 2009; Scott et al., 2007). The larvae of this line expressed Gal4 and activated UAS (upstream activating sequence)-mediated Kaede expression at the caudal tectum, and the rostro-medial URL on 1 and 2 dpf (Fig. 2N–Q), which is also when and where *atoh1a* is expressed (Suppl. Fig. 2). We marked the Kaede$^+$ cells at the rostro-medial URL by UV-mediated photoconversion at 24 hpf (Fig. 2R, T). The red (marked) cells lay at the rostral tip of the atoh1a:EGFP$^+$ domain just after the photoconversion, and they were detected in the Va and at the bottom of the cerebellum at 48 hpf (Fig. 2S, U, Suppl. Fig. 3). These cells extended their axons to the optic tectum or the hypothalamus (Fig. 2S, U) as observed in the atoh1a:EGFP line. Thus, our data show that the rostral-most group of cells derived from the *atoh1a*$^+$ progenitors migrates out of the cerebellum and generates the tegmental nuclei projecting to the optic tectum and the hypothalamus.

Generation of granule cells in cerebellum

Previous lineage tracing data show that *Atoh1*-expressing URL progenitors of the mouse cerebellum generate the granule cells (Machold and Fishell, 2005; Wang et al., 2005; Wilson and Wingate, 2006; Wingate, 2005). To investigate the possible transition of *atoh1*$^+$ URL progenitors to granule cells in the zebrafish cerebellum, we examined the expression of Neurod, which is expressed in immature and mature cerebellar granule cells in both mammals and zebrafish (Alder et al., 1996; Miyata et al., 1999; Mueller and Wullimann, 2002; Volkmann et al., 2008), and compared its expression with the atoh1a:EGFP signals.

First, we generated a monoclonal antibody against Neurod, and validated its specificity by showing comparable localization of *neurod* mRNA and the anti-Neurod immunoreactivity (Fig. 3A–D). Next, we verified Neurod's expression in granule cells. In sagittal sections at 3 dpf, most Neurod$^+$ cells were found in the superficial dorsal domain, and only a small population, in the mediolateral domain of the CCe, was detected deeper in the cerebellar tissue (arrow, Fig. 3Ba). At 5 dpf, Neurod$^+$ cells were detected below the Pvalb7$^+$ Purkinje cell layer (Fig. 3Da). Consistent with the previous report (Mueller and Wullimann, 2002), these data indicate that Neurod is expressed in both immature and mature granule cells, which are located in the dorsal superficial domain (molecular layer) and the granule cell layer, respectively. The Neurod signals overlapped with those of *vglut1* and *vglut2a*, which are markers of differentiated granule cells (data not shown).

In comparison with the atoh1a:EGFP expression pattern, we found that the Neurod signals overlapped with atoh1a:EGFP in the rostral CCe at 3 and 5 dpf (Fig. 3E, F), suggesting that the atoh1a:EGFP$^+$, Neurod$^+$ cells were in a transitional phase between the *atoh1a*$^+$ URL neuronal progenitor state and the immature granule cell state. Whereas Neurod$^+$ granule cells were detected throughout the molecular layer of the CCe (Fig. 3B, D), atoh1a:EGFP$^+$ Neurod$^+$ granule cells were detected only in the rostral molecular layer (Fig. 3E–G). We hypothesized that the *atoh1b*$^+$ and/or *atoh1c*$^+$ cells are neuronal progenitors that give rise to other Neurod$^+$ granule cells. Consistent with this, all of the atoh1a:EGFP$^+$, *atoh1b*$^+$, and *atoh1c*$^+$ cells incorporated bromodeoxyuridine (BrdU) in the early larval stages (Fig. 3H–J), indicating that the *atoh1a*$^+$, *atoh1b*$^+$, and *atoh1c*$^+$ cells are proliferating neuronal progenitors. Although we do not have transgenic lines for monitoring the progenies of the *atoh1b*$^+$ or *atoh1c*$^+$ progenitors, our data imply that *atoh1a*$^+$ and/or *atoh1b*$^+$ progenitors give rise to the granule cells in the rostral zebrafish cerebellum (Va and rostral CCe) and that the *atoh1c*$^+$ progenitors generate the granule cells of the caudal and lateral CCe, which correspond to the lobus caudalis cerebelli and the eminentia granularis, respectively.

Consistent with the previous report (Mueller and Wullimann, 2002), the Neurod$^+$ immature granule cells were proliferating at 3 and 5 dpf (Fig. 3K). Birthdate analysis revealed that the Neurod$^+$ immature granule cells in the molecular layer migrated to the granule cell layer between 5 and 7 dpf (Fig. 3L, M). All of these data suggest that during the early larval stages the neuronal progenitors expressing the *atoh1* genes generated the Neurod$^+$ immature proliferating granule cells that subsequently migrate into the granule cell layer and become the mature granule cells (Fig. 3N).

Development of GABAergic neurons and coordination with development of glutamatergic neurons

We next traced the GABAergic cell lineages by monitoring EGFP expression in *Tg(ptf1a:EGFP)* fish (Pisharath et al., 2007). As observed with *ptf1a* mRNA expression (Fig. 1O, P), ptf1a:EGFP was first detected in the cerebellar primordium at 2 dpf (Fig. 4A, B, E, F). Parvalbumin7 (Pvalb7), a marker for differentiated Purkinje cells (Bae et al., 2009), was first detected at 3 dpf and partly overlapped with the ptf1a:EGFP$^+$ domain (Fig. 4C), suggesting that Purkinje cells are descendants of the *ptf1a*$^+$ neuronal progenitors. At 5 dpf, the number of Pvalb7$^+$ Purkinje cells had increased and some of them were negative for ptf1a:EGFP (Fig. 4D). Sagittal sections showed ptf1a:EGFP signals in both the *ptf1a*$^+$ VZ cells and *ptf1a*$^-$ cells in the granule cell layer (Fig. 4I, J), confirming that the ptf1a:EGFP expression marked both the *ptf1a*$^+$ neuronal progenitors and their progenies. Only the ptf1a:EGFP$^+$ cells in the VZ but not those in the granule cell layer incorporated BrdU at 5 dpf (Fig. 4K), and the BrdU incorporated at 5 dpf was detected in Pvalb7$^+$ Purkinje cells at 7 dpf (Fig. 4L). These data identified three steps in GABAergic cell development: (1) *ptf1a*$^+$ neuronal progenitors proliferate in the VZ; (2) they stop proliferation, discontinue *ptf1a* expression, and start to migrate dorsally; and (3) they end their migration at a dorsal position corresponding to the Purkinje cell layer, where they differentiate into Purkinje cells, and probably into other GABAergic neurons (Fig. 4M).

We simultaneously monitored GABAergic and glutamatergic neuronal lineages, by detecting atoh1a:EGFP and ptf1a:Gal4VP16; UAS:NfsB-mCherry (ptf1a:G4-U:mCherry, Fig. 5). In the 2-dpf embryo, atoh1a:EGFP$^+$ and ptf1a:G4-U:mCherry$^+$ cells were, respectively, located exclusively in the rostral and caudal cerebellar primordium (Fig. 5A, D). During the early larval stages (3 to 5 dpf, Fig. 5B, C, E, F), the atoh1a:EGFP$^+$ cell lineages migrated into the granule cell layer; the ptf1a:mCherry$^+$ lineages expanded rostrally and migrated dorsally into the Purkinje cell layer (Fig. 5I). These data suggest that these morphogenetic processes, including the

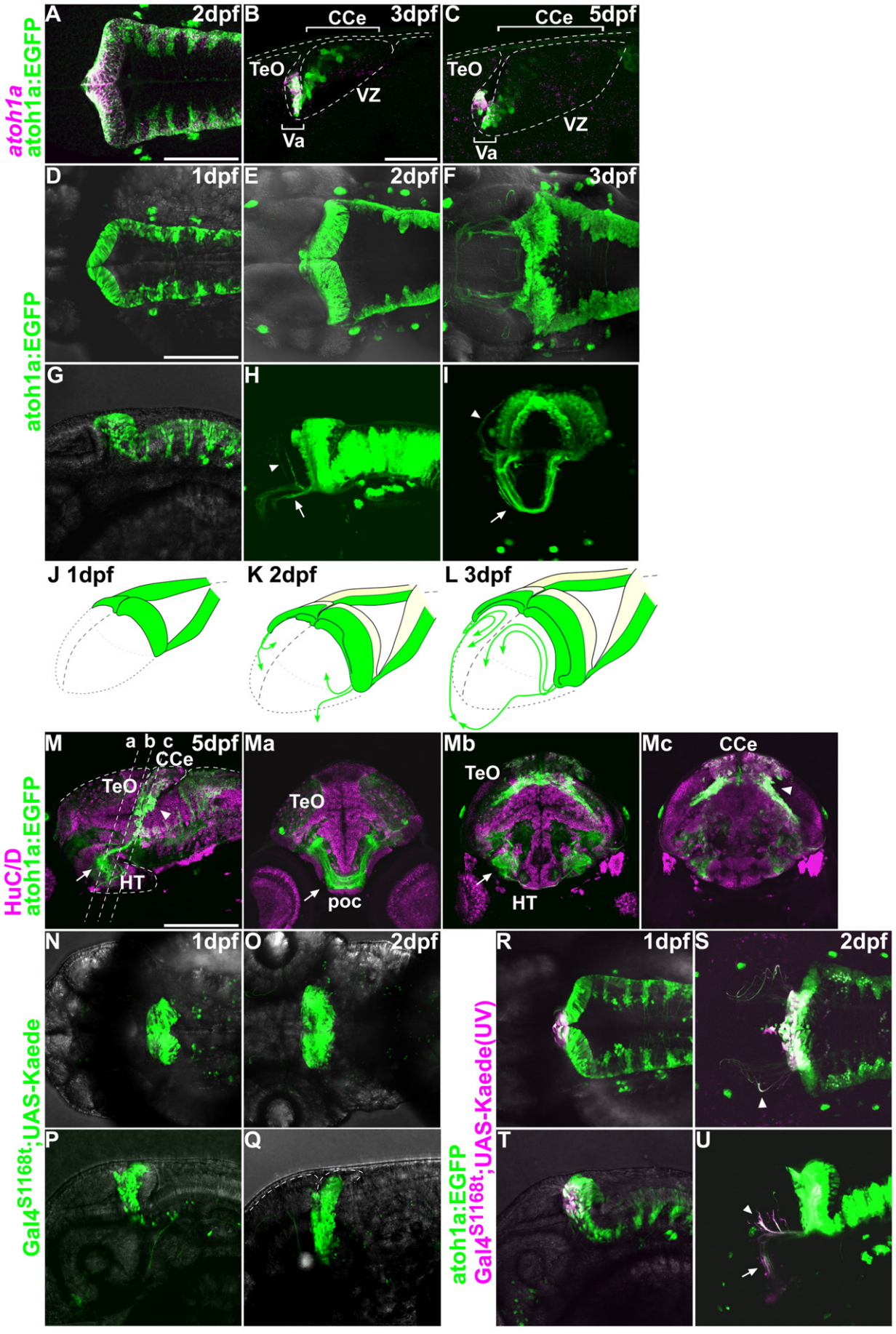
atoh1a
atoh1a:EGFP
A 2dpf
B CCe 3dpf
C CCe 5dpf
TeO
VZ
Va
D 1dpf
E 2dpf
F 3dpf
atoh1a:EGFP
G
H
I
J 1dpf
K 2dpf
L 3dpf
HuC/D
atoh1a:EGFP
M a b c 5dpf
CCe
TeO
HT
Ma
TeO
poc
Mb
TeO
HT
Mc
CCe
Gal4S1168t;UAS-Kaede
N 1dpf
O 2dpf
P
Q
atoh1a:EGFP
Gal4S1168t;UAS-Kaede(UV)
R 1dpf
S 2dpf
T
U

contributions of the *atoh1b*$^+$ and *atoh1c*$^+$ cell lineages to the granule cells, lead to the formation of the cerebellar layers at 5 dpf (Fig. 5I, J).

Development of olig2$^+$ *eurydendroid cells*

In larval and adult fish, a population of cerebellar projection neurons, called eurydendroid cells, expresses the marker *olig2* (Bae et al., 2009; McFarland et al., 2008). As reported (McFarland et al., 2008), olig2:EGFP signals recapitulated the expression of *olig2* mRNA at the embryonic and early larval stages (Fig. 6A–F). Many *olig2*$^+$ cells that were located distal to the VZ were also positive for vglut2a:DsRed at 3 (44/51, from three paramedian slices in an embryo) and 5 dpf (56/63, from three paramedian slices in a larva; arrows, Fig. 6G–J; similar results were observed from ten other samples). Since olig2:EGFP$^+$ cells include undifferentiated eurydendroid cells and oligodendrocytes (Bae et al., 2009), most if not all of the olig2:EGFP$^+$ neurons are glutamatergic. We also detected olig2:EGFP$^+$ cells in the VZ of the larval cerebellum (arrowheads, Fig. 6H, J), indicating that olig2:EGFP marks both neuronal progenitors and differentiated *olig2*$^+$ eurydendroid cells. To address whether the *olig2*$^+$ eurydendroid cells are derived from the *ptf1a*$^+$ or *atoh1*$^+$ neuronal progenitors, we compared olig2:EGFP signals with ptf1a:G4-U:mCherry or atoh1a:dTomato signals. At 2 dpf, most of the olig2:EGFP signals were detected in ptf1a:G4-U:mCherry$^+$ cells in the VZ (51/66 in a larva, similar results were seen in more than ten larvae; Fig. 6K, L). At 5 dpf and in adults, the olig2:EGFP$^+$ signals were detected in ptf1a:G4-U:mCherry$^+$ cells in the caudal VZ (5 dpf: 21/21 from four slices, $n=2$; Fig. 6M–O). We further compared signals of olig2:EGFP and atoh1a:dTomato, which showed similar expression to atoh1a:EGFP (data not shown). We found that a minor population of olig2:EGFP$^+$ cells was positive for atoh1a:dTomato at 2 dpf (5/50 from two slices in an embryo, similar results were obtained in ten embryos), and the olig2:EGFP$^+$, atoh1a:dTomato$^+$ cells were located near the lateral edge of the VZ (Fig. 6P, Q). The olig2:EGFP$^+$, atoh1a:dTomato$^+$ cell population had expanded at 5 dpf (13/96 from two slices in a larva; arrows, Fig. 6Q, S; similar results were seen in more than ten larvae). These data suggest that the *olig2*$^+$ eurydendroid cells are derived from progenitors located in the caudal VZ and the lateral regions of the URL, which correspond to *ptf1a*$^+$ and *atoh1a*$^+$ progenitor domains, respectively (Fig. 6T). Although the *olig2*$^+$ eurydendroid cells are derived from both VZ and URL progenitors, they are glutamatergic neurons.

Proneural genes mark adult neural progenitor cells

Neurogenesis takes place continuously in the adult zebrafish cerebellum (Ekström et al., 2001; Grandel et al., 2006; Zupanc et al., 2005). In an attempt to reveal whether proneural gene expression is linked to adult neurogenesis, we examined the expression of the proneural genes in the late larval, juvenile, and adult cerebellum (Fig. 7). At early (Fig. 1E) and late larval (Fig. 7A) stages, *atoh1a* expression was detected in the molecular layer of the Va (Fig. 7G); in the adult, was confined to the rostral-most tip of the Va (Fig. 7K). *atoh1b* and *atoh1c* were detected in the molecular layer of the Va and CCe midline from the larval through the adult stages (Fig. 7B, C, E, H, I, L, M, O, P). From the embryonic through the adult stages (Figs. 1P–V, 7D, F, J, N, Q), *ptf1a* was continuously detected in the VZ adjacent to the cerebral aqueduct and the fourth ventricle; *ptf1a* expression was stronger in the juxta-medial VZ than the midline VZ; it was also detected near and in the Purkinje cell layer (Fig. 7D, F, J). Thus, in the adult zebrafish cerebellum, *atoh1*$^+$ cells are located in the molecular layer of the Va and medial CCe, and *ptf1a*$^+$ cells are located in the VZ (Fig. 7R).

We next addressed whether the expression of the proneural genes was linked to adult neurogenesis (Fig. 8). As reported previously (Grandel et al., 2006; Kaslin et al., 2009; Zupanc et al., 2005), many proliferating cells (i.e., cells that incorporated BrdU) were located in the molecular layer of the Va and CCe midline (Fig. 8A–C). Further examination showed that all of the atoh1a:EGFP$^+$, *atoh1b*$^+$, and *atoh1c*$^+$ cells were BrdU$^+$ proliferating cells (Fig. 8A–C), suggesting that the *atoh1* genes mark glutamatergic neuronal progenitors in the adult cerebellum. Furthermore, we found that many Neurod$^+$ granule cells in the adult molecular layer, but not the granule cell layer, incorporated BrdU (88/232, $n=4$, Fig. 8D), and most of the BrdU-labeled cells were detected in the granule cell layer 5 days after the labeling (Fig. 8E). Thus, the Neurod$^+$ immature granule cells of the adult cerebellum, which are derived from the *atoh1*$^+$ neuronal progenitors, proliferate in the molecular layer, but stop their proliferation and migrate into the granule cell layer within 5 days.

In the VZ of adults, a substantial number of cells incorporated BrdU, although there were fewer proliferating cells than in zebrafish larvae (Fig. 8F, Fa). All of the BrdU$^+$ cells in the VZ were ptf1a:EGFP$^+$ (arrows, Fig. 8F), indicating that these cells are neuronal progenitors for GABAergic neurons. We detected BrdU incorporation in a small population of the Pvalb7$^+$ Purkinje cells 5 days after the labeling (Fig. 8H), suggesting that the *ptf1a*$^+$ neuronal progenitors gave rise to Purkinje cells in the adult cerebellum. However, the number of BrdU-incorporated cells that differentiated into Purkinje cells was far less than the number that became granule cells (Fig. 8H), suggesting a slow turnover of GABAergic neuronal lineage.

In the adult mammalian telencephalon and cerebellum, Blbp (brain lipid-binding protein, also called Fabp7)-expressing glial cells are known to be neural precursors (Hartfuss et al., 2001; Malatesta et al., 2003, 2000; Pinto and Gotz, 2007; Ponti et al., 2008). Therefore, we investigated whether Bergmann glial cells proliferate in the adult zebrafish cerebellum. Co-staining for incorporated BrdU and *blbp* transcripts showed that at least some of the Blbp$^+$ Bergmann glial cells were proliferating, and therefore act as neural progenitors (Fig. 8I). Our findings demonstrate that neurogenesis takes place continuously in the molecular layer and VZ of the adult zebrafish cerebellum, and the proneural genes *atoh1a, b, c* and *ptf1a* mark at least some of the adult neuronal progenitors.

Discussion

In this study, we analyzed the expression of proneural genes in the zebrafish cerebellum during the embryonic, larval, and adult stages and compared their expression patterns with those of known markers of proliferation and differentiation. We used transgenic lines for lineage tracing as expression of the fluorescent proteins continued for

Fig. 2. Behaviors of neurons derived from *atoh1a*$^+$ neuronal progenitors. (A–C) Expression of *atoh1a* mRNA (magenta) and EGFP (atoh1a:EGFP, green) in the cerebellum of *Tg (atoh1a:EGFP)* fish at 2, 3, and 5 dpf. Dorsal view (A) and parasagittal sections (B, C), with rostral to the left. Note that the atoh1a:EGFP signals overlap those of the *atoh1a* transcripts at 2 dpf in the valvula cerebelli (Va) but not the corpus cerebelli (CCe). The *atoh1a*$^-$, atoh1a:EGFP$^+$ cells are descendants of *atoh1a*$^+$ progenitors. (D–J) Expression of atoh1a:EGFP at 1 (D, G), 2 (E, H), and 3 dpf (F, I). Dorsal (D–F), lateral (G, H), antero-lateral (I) views. Arrows and arrowheads indicate axonal projections to the optic tectum and hypothalamus, respectively (H, I). (J-L) Schematic representation of atoh1:EGFP$^+$ cells and their projections at 1 (J), 2 (K), and 3 dpf (L). (M) Expression of atoh1a:EGFP (green) and HuC/D (magenta) at 5 dpf. Sagittal section (M). (Ma, b, c) Cross sections at the levels indicated in (M). Arrows indicate tegmental nuclei derived from the URL, which include secondary gustatory nucleus (SGN). Projections from the atoh1a:EGFP$^+$ SGN are indicated by arrowheads. (N–U) Lineage tracing of the rostro-medial *atoh1a*$^+$ cells using the photoconvertible protein Kaede. Green (non-photoconverted) Kaede was detected in the rostral cerebellum in *Et(fos:Gal4-VP16)s1168t; Tg(UAS-E1b: Kaede)s1999t* at 1 (N, P) and 2 dpf (O, Q). The tectum and cerebellum are indicated by dotted lines (Q). The green fluorescent Kaede in the rostro-medial cerebellum was converted to a red fluorescent protein (magenta) by UV irradiation at 24 hpf in *Et(fos:Gal4-VP16)s1168t; Tg(UAS-E1b: Kaede)s1999t; Tg(atoh1a:EGFP)* (R-U). The Kaede expression overlapped with that of atoh1a:EGFP in the rostro-medial cerebellum (R, T, and Suppl. Fig. 2). These rostro-medial cells migrated ventro-laterally (S, U, and Suppl. Fig. 3) were located at the bottom of the cerebellum, and projected to the optic tectum (arrowheads) and hypothalamus (arrow). These cells were located in the tegmentum at 5 dpf (M). HT, hypothalamus; poc, postoptic commissure. Other abbreviations are the same as in Fig. 1. Scale bars: 100 μm (B, D), 200 μm (M).

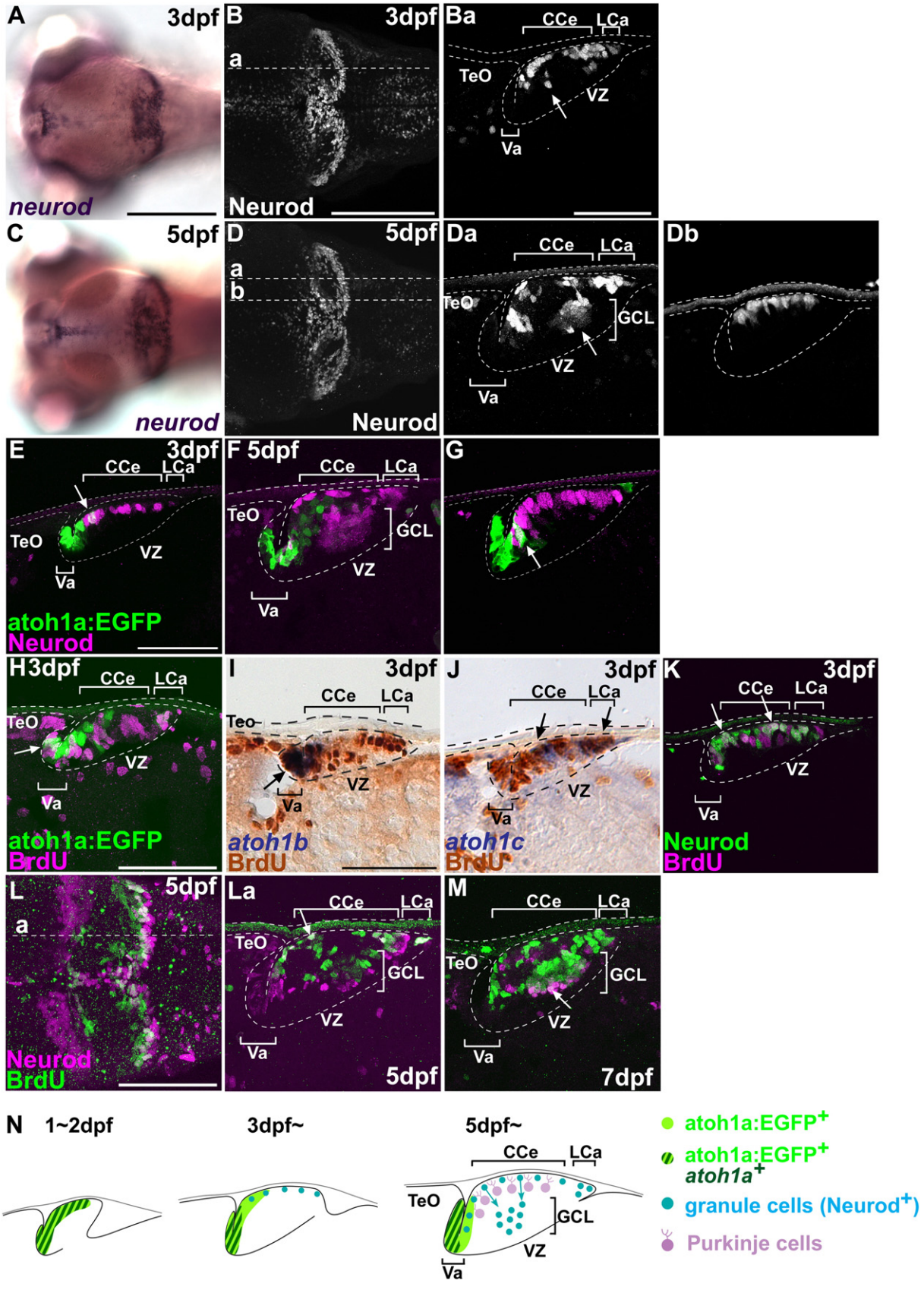
A 3dpf
neurod
B 3dpf
a
Neurod
Ba
CCe
LCa
TeO
VZ
Va
C 5dpf
neurod
D 5dpf
a
b
Neurod
Da
GCL
Db
E 3dpf
atoh1a:EGFP
Neurod
F 5dpf
G
H3dpf
atoh1a:EGFP
BrdU
I 3dpf
atoh1b
BrdU
J 3dpf
atoh1c
BrdU
K 3dpf
Neurod
BrdU
L 5dpf
La
5dpf
M
7dpf
N 1~2dpf
3dpf~
5dpf~
atoh1a:EGFP+
atoh1a:EGFP+
atoh1a+
granule cells (Neurod+)
Purkinje cells

a long period after the disappearance of the proneural gene expression, enabling us to trace the fate of the cerebellar cells that originated from the proneural gene-expressing progenitors. The length of time the florescent proteins could be detected, however, was dependent on the cell types and cell conditions. The fluorescent proteins could be diluted in cells that proliferate rapidly, such as the granule cells. If it takes cells a long period to migrate and become differentiated, the fluorescent proteins may no longer be detected in the differentiated neurons (e.g. Purkinje cells). Nevertheless, the expression of the fluorescent proteins in the transgenic lines could mark the progenitors expressing the proneural genes and the neurons that were newly differentiated from the progenitors. Our findings with the transgenic fish-mediated lineage tracing revealed that the proneural gene-linked neurogenesis in the cerebellum is well conserved between zebrafish and mammals. We also found that the zebrafish cerebellum exhibits neurogenic features that are apparently unique to teleosts: the development of eurydendroid cells and adult cerebellar neurogenesis.

Rostral migratory streams of atoh1$^+$ URL progenies

Lineage tracing in the mouse cerebellum using the *Math1-CreER^{T2}* transgenic line or *Math1^{LacZ}* knock-in line revealed that *Atoh1$^+$* (*Math1$^+$*) neuronal progenitors in the hindbrain sequentially generate the glutamatergic neurons that are located within or outside of the cerebellum (Machold and Fishell, 2005; Wang et al., 2005). The first group of progeny derived from the *Atoh1$^+$* URL progenitors migrates rostro-ventrally then exits the cerebellum (rostral rhombic-lip migratory stream) to form multiple nuclei in the tegmentum (Machold and Fishell, 2005; Wang et al., 2005; Wilson and Wingate, 2006; Wingate, 2005). A similar rostro-ventral migration of the URL cells was previously reported in zebrafish (Köster and Fraser, 2001). In this report, using lineage tracing with *Tg(atoh1a:EGFP)* and an enhancer trap line, we showed that a portion of the rostral-most cells that derived from *atoh1a$^+$* progenitors migrated out of the cerebellum into the tegmentum. Therefore, the rostral migratory stream from the URL is conserved in zebrafish (Fig. 2). In mice, the tegmental nuclei derived from *Atoh1$^+$* progenitors include the parabrachial nuclei that function to integrate proprioceptive and vestibular inputs with autonomic functions (Balaban et al., 2002), and cholinergic nuclei that project to the thalamus or other brain regions and interact with the dopaminergic system (Yeomans, 1995). The tegmental nuclei derived from the *atoh1a$^+$* neuronal progenitors in zebrafish include the secondary gustatory nuclei (Fig. 2 and Suppl. Fig. 1), and they project their axons to the optic tectum and the hypothalamus in zebrafish (Fig. 2), suggesting that the roles of these tegmental nuclei are in modifying the autonomous function or the visual system. Future functional studies of the tegmental nuclei in zebrafish will reveal whether the URL-derived tegmental nuclei have conserved functions in vertebrates.

Contribution of URL-derived progenies to granule cells

A recent report on a transgenic zebrafish line (gata1:GFP) that expresses GFP in the granule cell lineage revealed that the descendents of the dorsomedial URL progenitors migrate rostrally and generate the granule cells of the CCe; descendents of the lateral URL progenitors remain in place and form the granule cells of the eminentia granularis and the lobus caudalis cerebelli (Volkmann et al., 2008). Here we re-assessed the contribution of the medial URL progenitors to the granule cells of the CCe using the *Tg(atoh1a:EGFP)* line and our results added important details to previous findings. We found that, first, the atoh1a:EGFP$^+$ cells migrated rostrally (Fig. 1 and Suppl. Movie 1). Second, the cells positive for atoh1a:EGFP$^+$ and the granule cell marker Neurod appeared in the superficial domain of the medial and mediolateral CCe (Fig. 2E–G). Third, by birthdate analysis, we found that proliferating Neurod$^+$ immature granule cells in the superficial domain stopped their proliferation and left the superficial domain for the granule cell layer (Fig. 2L, M). This is consistent with the previous report (Mueller and Wullimann, 2002) demonstrating that HuC/D-positive mitotic neurons are derived from the progenitor zone of the external granule cell layer. Furthermore, the location of the proliferating and non-proliferating Neurod$^+$ granule cells indicates that the Neurod$^+$ cell domains in the molecular and granule cell layers, respectively, correspond to the mammalian external granule cell layer and internal granule cell layer. Our findings also show that there are conserved steps between zebrafish and mammals in the generation of granule cells: *atoh1$^+$* neuronal progenitors in the external granule cell layer>Neurod$^+$ proliferating granule cells in the external granule cell layer>Neurod$^+$ mature granule in the internal granule cell layer.

It has recently been reported that although *atoh1*-expressing cells are located along the midline of the cerebellum, they migrate quickly and do not exhibit a transit amplification of the granule cells in zebrafish cerebellum, arguing that the zebrafish cerebellum does not have the external germinal layer (Chaplin et al., 2010). However, we found that *atoh1a, atoh1b*, or *atoh1c*-expressing progenitors and Neurod$^+$ immature granule cells in the molecular layer of the Va and the CCe midline could incorporate BrdU, and are thus proliferating cells (Fig. 3), as observed in the external granule cell layer of the mammalian and avian cerebellums (Wingate, 2001). Therefore, although the proneural gene-expressing cells may not be identical to the cells in the external granule cell layer of the mammalian cerebellum (e.g. a layered structure, Sonic hedgehog dependency), they share similar characteristics with the cells in the external granule cell layer.

In contrast to *atoh1a*, *atoh1b* and *atoh1c* are expressed in the medial external granule cell layer and caudal CCe (Fig. 1I, J, M, N). Cells expressing *atoh1b* and *atoh1c* proliferated during the early larval stages, as *atoh1a*-expressing cells did (Fig. 3H–J). Since Neurod$^+$ proliferating granule cells were located in these regions (Fig. 3L), our data suggest that the *atoh1b$^+$* and/or *atoh1c$^+$* neuronal progenitors in the caudal domain of the CCe give rise to the granule cells of the eminentia granularis and the lobus caudalis cerebelli. Lineage tracing of the progenies of the *atoh1b$^+$* and *atoh1c$^+$* progenitors will resolve this issue. We previously reported that the granule cells in the CCe and the lobus caudalis cerebelli express a different set of genes (Bae et al., 2009). It is reported that these granule cells construct distinct neuronal circuits (Volkmann et al., 2008). It is tempting to speculate that the fate of granule cells is determined by genetic programming: that is, the *atoh1a$^+$* and/or *atoh1b$^+$* progenitors produced granule cells in the Va and CCe, and the *atoh1b$^+$* and/or *atoh1c$^+$* progenitors generate granule cells in the lobus caudalis cerebelli and possibly the

Fig. 3. Behavior of granule cells. (A–D) Expression of *neurod* at 3 (A, B) and 5 (C, D) dpf. Dorsal views (A, B, C, D) and sagittal sections at the levels indicated in B and D (Ba, Da, Db). Neurod$^+$ mature granule cells in the granule cell layer are marked by arrows. (E, F) Expression of atoh1a:EGFP (green) and Neurod (magenta) at 3 (E) and 5 dpf (F, G). Sagittal sections at the levels comparable to Ba (for E), Da (for F), and Db (for G). atoh1a:EGFP$^+$ Neurod$^+$ cells are marked by arrows. (H–K) BrdU incorporation at 3 dpf. *Tg(atoh1a:EGFP)* (H) or wild-type larvae (I–K) were labeled with bromodeoxyuridine (BrdU) for 1 h, and proliferating cells were analyzed by immunostaining with anti-BrdU (magenta in H and K; brown in I and J) antibody, and anti-EGFP (green, H), anti-Neurod (green, K) antibodies, *atoh1b* (I) or *atoh1c* (J) riboprobes. Sagittal sections. The larvae were stained with anti-BrdU (magenta) and anti-Neurod (green) antibodies. Cells that were positive both for BrdU signals and proneural gene expression are marked by arrows. (L, M) Birthdate analysis. Larvae were labeled with BrdU at 5 dpf and fixed 1 h after the labeling (L) or at 7 dpf (two days after the labeling, M). Dorsal view (L) and sagittal sections at the mediolateral level (La and M). BrdU$^+$ Neurod$^+$ cells are marked by arrows. (N) Schematic representation of granule cell development during the larval period. TeO, tectum opticum; GCL, granule cell layer; other abbreviations are described in Fig. 1. Scale bars: 50 μm (Ba, E, H), 100 μm (L), 200 μm (A, B).

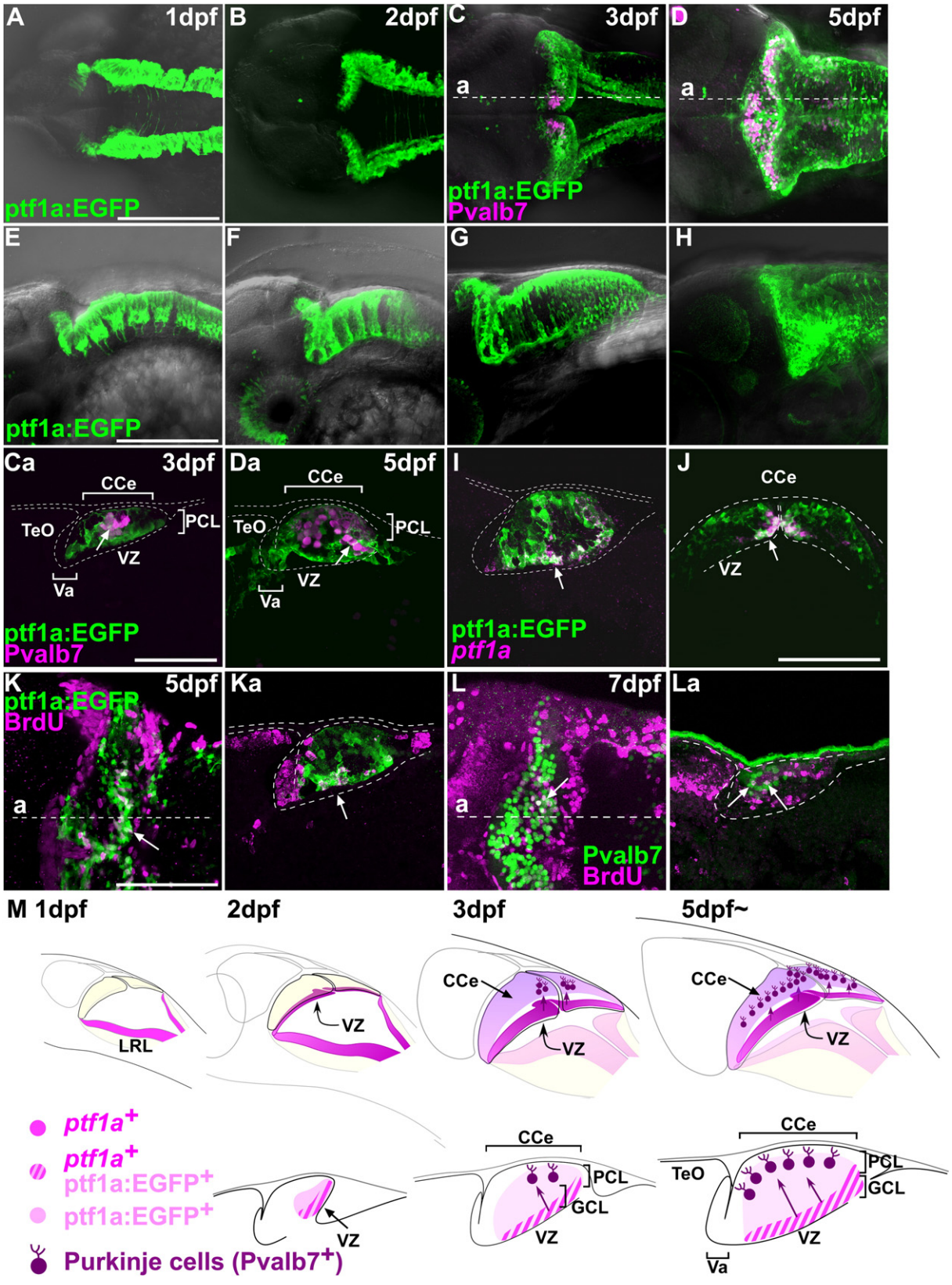

Fig. 4. Differentiation and migration of GABAergic neurons. (A–H) Expression of ptf1a:EGFP (green) and Pvalb7 (magenta) in the cerebellum at 1, 2, 3, and 5 dpf. Dorsal views (A–D), lateral views (E–H) with rostral to the left. (Ca, Da) Parasagittal sections at the levels indicated in (C) and (D). Note that many cells were positive for both ptf1a:EGFP and Pvalb7 (arrows, Ca, Da) (I, J) Parasagittal (I) and cross-sectional (J) views showing the expression of *ptf1a* mRNA (magenta) and ptf1a:EGFP (green) at 5 dpf. Most cells in the VZ were both *ptf1a*$^{+}$ and ptf1a:EGFP^{+} (arrows). *ptf1a*$^{-}$ ptf1a:EGFP^{+} cells found superficial to the VZ were immature neurons derived from the *ptf1a*$^{+}$ neural progenitors in the VZ. (K) BrdU incorporation. *Tg(ptf1a:EGFP)* fish were labeled with BrdU at 5 dpf for 1 h, and proliferating cells were analyzed by immunostaining with anti-BrdU (magenta) and anti-EGFP (green) antibodies. Dorsal stacking view (K) and parasagittal section (Ka) are shown. BrdU signals were detected in ptf1a:EGFP^{+} cells in the VZ (arrows). (L) Birthdate analysis. Larvae were labeled with BrdU at 3 dpf and fixed at 7 dpf. The larvae were stained with anti-BrdU (magenta) and anti-Pvalb7 (green) antibodies. Dorsal stacking view (L) and parasagittal section (La) are shown. Note that BrdU signals were detected in Pvalb7^{+} Purkinje cells (arrows). (M) Schematic representation of development of GABAergic neurons. PCL, Purkinje cell layer; other abbreviation is described in Figs. 1 and 3. Scale bars: 50 μm (Ca, J), 100 μm (K), 200 μm (A, E).

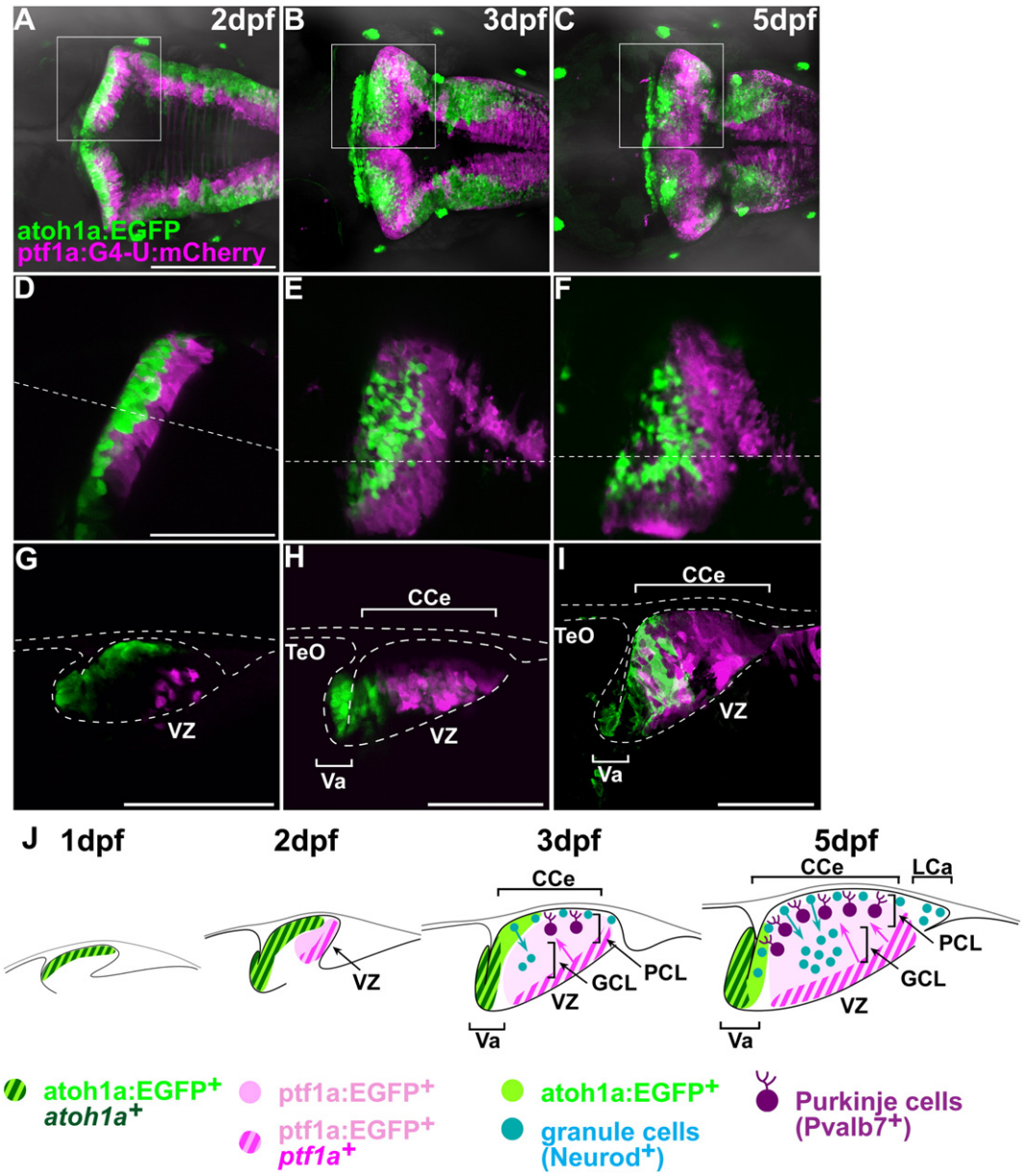

Fig. 5. Coordinated migration and expansion of glutamatergic and GABAergic neurons in the larval cerebellum. (A–I) Tracing of the glutamatergic and GABAergic lineages. *Tg(UAS-E1b:NfsB-mCherry); Tg(ptf1a:Gal4VP16)* fish (*Tg(ptf1a:G4-U:mCherrry)*) were crossed with *Tg(atoh1a:EGFP)* to mark the lineages of cells derived from *atoh1a*$^+$ or *ptf1a*$^+$ neuronal progenitors. The expression of EGFP (glutamatergic lineage) and mCherry (GABAergic lineage) was analyzed on dpf 2 (A, D, G), 3 (B, E, H), and 5 (C, F, I). Dorsal stacking views with rostral to the left (A-F), and lateral views of optical sections (G, H), and a histological section (I) are shown. (J) Schematic representation of the development of the two lineages. At 2 dpf, *atoh1a*$^+$ glutamatergic and *ptf1a*$^+$ GABAergic progenitors occupy, respectively, the anterior and posterior domains, of the cerebellum. From 3 to 5 dpf, *atoh1a*$^+$ progenitors generate atoh1a:EGFP$^+$ granule cells in the ML, which become Neurod$^+$ immature granule cells and migrate to the granule cell layer; ptf1a:EGFP$^+$ cells migrate dorsally from the VZ and become differentiated into Purkinje cells at the Purkinje cell layer. These processes generate the three cerebellar layers visible at 5 dpf. The abbreviations are defined in Figs. 1, 3, and 4. Scale bars: 50 μm (G, H, I), 100 μm (D), 200 μm (A).

eminentia granularis. This is consistent with the finding that granule cells in the CCe, the eminetia granularis, and the lobus caudalis cerebella take distinct trajectories in their migration (Volkmann et al., 2008). Our data suggest that distinct genetic programs control the generation of the granule cells in different domains and may contribute to the functional diversity of the mature granule cells.

Coordinated development of Purkinje cells and granule cells

The VZ generates the Purkinje cells and other classes of cerebellar interneurons (Altman and Bayer, 1997). Mouse genetic analyses show that the *Ptf1a*$^+$ neuronal progenitors in the VZ are the source of all GABAergic neurons in the mouse cerebellum, including the Purkinje, Golgi, and stellate cells (Hoshino, 2006; Hoshino et al., 2005). Here, using the *Tg(ptf1a:EGFP)* line, we found ptf1a:EGFP signals in both the VZ progenitors and their progenies and in newly differentiated Purkinje cells (Fig. 4C, D). These data strongly suggest that Purkinje cells are generated by the *ptf1a*$^+$ VZ progenitors in the zebrafish as well as the mouse cerebellum. It is not clear yet whether all Purkinje cells are derived from the *ptf1a*$^+$ VZ progenitors or whether the same progenitors also generate other GABAergic neurons, as reported for the mammalian cerebellum (Hoshino et al., 2005). However, considering the conserved gene expression and migration of the VZ-derived cells, GABAergic interneurons are also likely produced by *ptf1a*$^+$ progenitors in the zebrafish VZ. Future long-term lineage analysis, using techniques such as the Cre-loxP system to label the descendents of the VZ progenitors in zebrafish, may clarify how the *ptf1a*$^+$ cells generate a diverse set of GABAergic neurons.

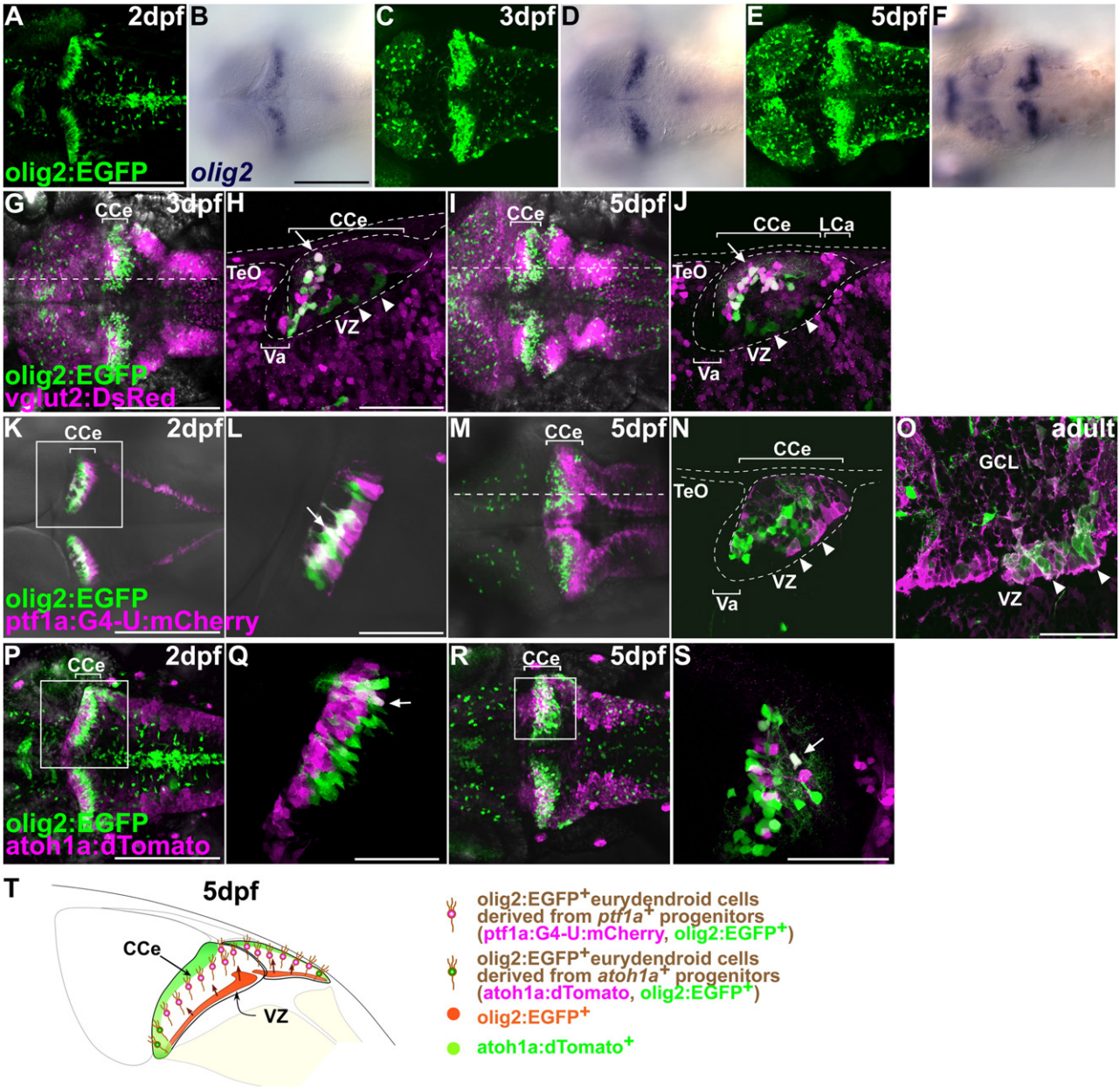

Fig. 6. Differentiation and migration of *olig2*$^+$ eurydendroid cells. (A–F) Expression of *olig2* (B, D, F) and olig2:EGFP (A, C, E) in the cerebellum at 2, 3, and 5 dpf. Dorsal views with rostral to the left. (G–J) Expression of olig2:EGFP and vglut2:DsRed at 3 (G, H) and 5 (I, J) dpf. EGFP and DsRed signals in *Tg(olig2:EGFP); Tg(vglut2a:DsRed)* were detected with anti-EGFP (green) and anti-DsRed (magenta) antibodies, respectively. (H, J) Sagittal sections at the levels indicated in G and I, respectively. The olig2:EGFP$^+$ cells in the VZ were negative for vglut2a:DsRed (arrowheads), but in the GCL and PCL domains, most olig2:EGFP$^+$ cells were positive for vglut2a:DsRed (arrows). (K–O) Expression of olig2:EGFP and ptf1a:Gal4VP16; UAS:NfsB-mCherry (ptf1a:G4-U:mCherry) at 2 dpf (K, L), 5 dpf (M, N), and the adult cerebellum (O). (K, M) Dorsal views; (L) high-magnification view of the box in (K); (N) sagittal section at the level indicated in (M); (O) sagittal section. Note that most olig2:EGFP$^+$ cells were also positive for ptf1a:G4-UAS:mCherry at 2 dpf (arrows), but many of them became negative after differentiation at 5 dpf. olig2:EGFP$^+$ ptf1a:G4-U:mCherry$^+$ cells were also detected in the VZ at 5 dpf and adult stage (arrowheads). (P-S) Expression of olig2:EGFP and atoh1a:dTomato at 2 (P, Q) and 5 (R, S) dpf. (Q, S) High-magnification views of the boxes in (P, R). The olig2:EGFP$^+$ cells located in the lateral domains were positive for atoh1a:dTomato (arrows). (T) Schematic representation of development of the *olig2*$^+$ eurydendroid cells. The abbreviations are defined in Fig. 1. Scale bars: 50 μm (H, S), 100 μm (L), 200 μm (A, B, G, K, O, P).

Chick-quail chimera experiments (Alvarez Otero et al., 1993; Hallonet et al., 1990) and clonal analyses in the mammalian cerebellum (Mathis et al., 1997; Mathis and Nicolas, 2003; Zhang and Goldman, 1996) revealed that the neurons in the molecular layer derive from the VZ and are produced by dividing progenitors located in the granule cell layer in these species. However, in the zebrafish cerebellum, we found that only the ptf1a:EGFP$^+$ cells in the VZ, but not those in the granule cell layer, could incorporate BrdU at the larval and adult stages (Figs. 4K, 8F), indicating that the *ptf1a*$^+$ cells in the VZ are only proliferating progenitors for the GABAergic neurons, and the cells migrating from the VZ do not proliferate. Although there were a few proliferating (i.e., BrdU-incorporating) cells detected near the VZ in the granule cell layer of the adult zebrafish cerebellum, these cells were negative for ptf1a:EGFP signals (Fig. 8F), implying they were not GABAergic-lineage cells.

In the mouse, labeling dividing cells with an adenoviral vector showed that proliferating cells are located in the VZ but not the marginal zone (above the VZ) at the beginning of cerebellar formation (embryonic day 11.5) (Hashimoto and Mikoshiba, 2003). Therefore, in the zebrafish cerebellum and the early embryonic-stage mouse cerebellum, *ptf1a*$^+$ VZ progenitors are proliferating; they stop expressing *ptf1a* and end their proliferation when they leave the VZ.

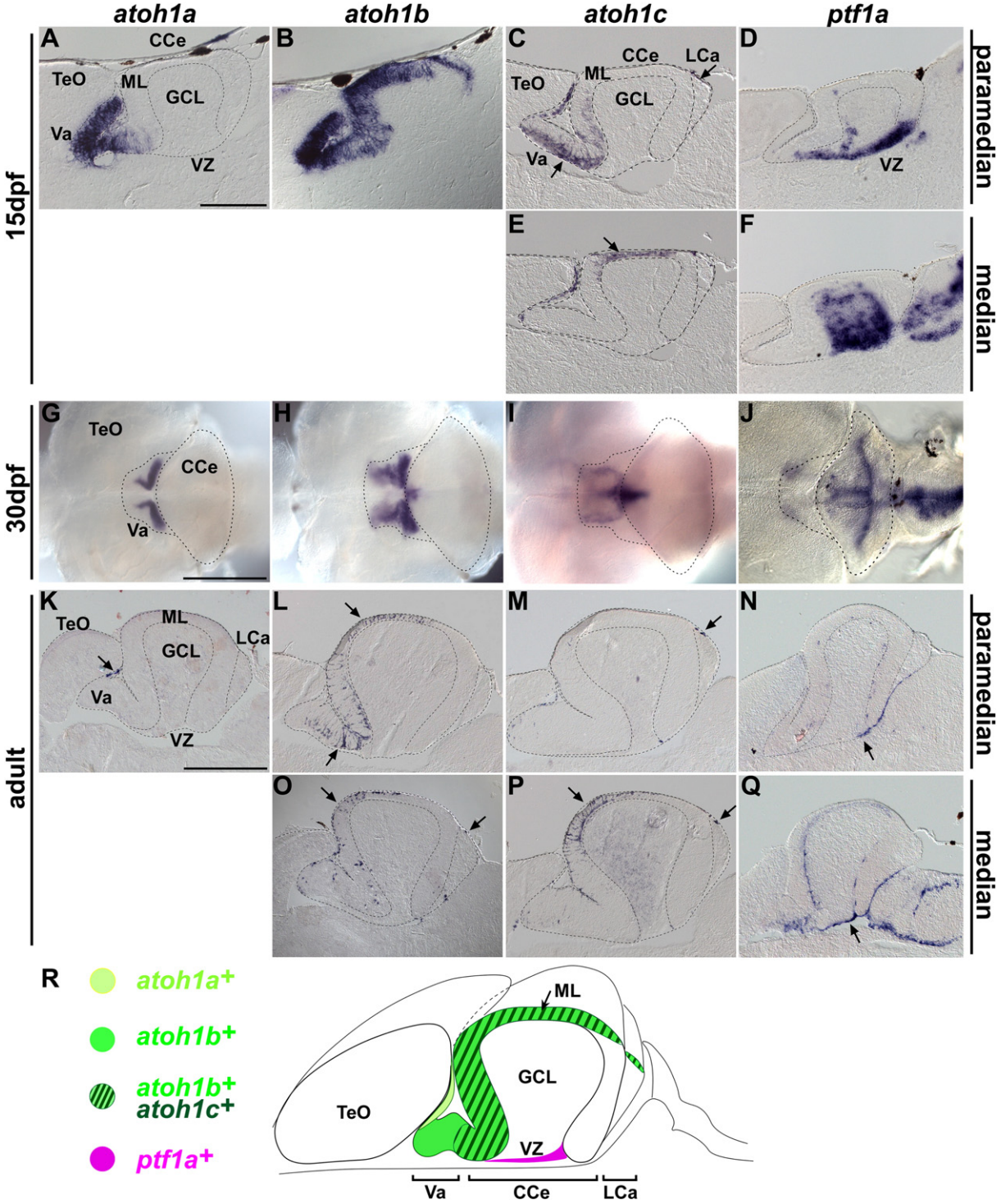

Fig. 7. Expression of proneural genes in juvenile and adult cerebellum. Expression of *atoh1a*, *atoh1b*, *atoh1c*, and *ptf1a* in cerebellum at late larval (15 dpf, A–F), juvenile (30 dpf, G–J), and adult (90 dpf or older, K–Q) stages by in situ hybridization. Sagittal sections, at paramedian (A–D, K–N) or median (E, F, O–Q) levels. Whole-mount in situ hybridization with dorsal views (G–J). Note that the expression domains of *atoh1b* and *atoh1c* in the midline are very thin, and were not detected by whole mount in situ hybridization (H, I). (R) Schematic representation of *atoh1a*, *atoh1b*, *atoh1c*, and *ptf1a* expression in the adult cerebellum. The abbreviations are defined in Figs. 1 and 3. Scale bars: 100 μm (A), 500 μm (G), 1 mm (K).

Pvalb7 was detected only in the dorsal superficial domain of the cerebellum, which corresponds to the Purkinje cell layer, at larval and adult stages in the zebrafish (Figs. 4C, L, 8H) (Bae et al., 2009), indicating that the Purkinje cell progenitors (*ptf1a*$^{-}$ ptfa1:EGFP^{+} cells) differentiate after they reach the Purkinje cell layer.

In addition to *ptf1a*, *ascl1a* (*zash1a*) is reported to be expressed in the VZ of the larval cerebellum (Wullimann and Mueller, 2002), suggesting the role of *ascl1a* in generating GABAergic neurons. It will be intriguing to elucidate whether *ascl1a* functions downstream of *ptf1a*, or *ascl1a* and *ptf1a* cooperatively function to generate the GABAergic neurons. Future studies will clarify this issue.

By monitoring atoh1a:EGFP^{+} and ptf1a:G4-U:mCherry^{+} cells, we found that the *atoh1a*$^{+}$ and *ptf1a*$^{+}$ lineages are adjacent to one another with little or no gap between them in the cerebellar primordium at 2 dpf

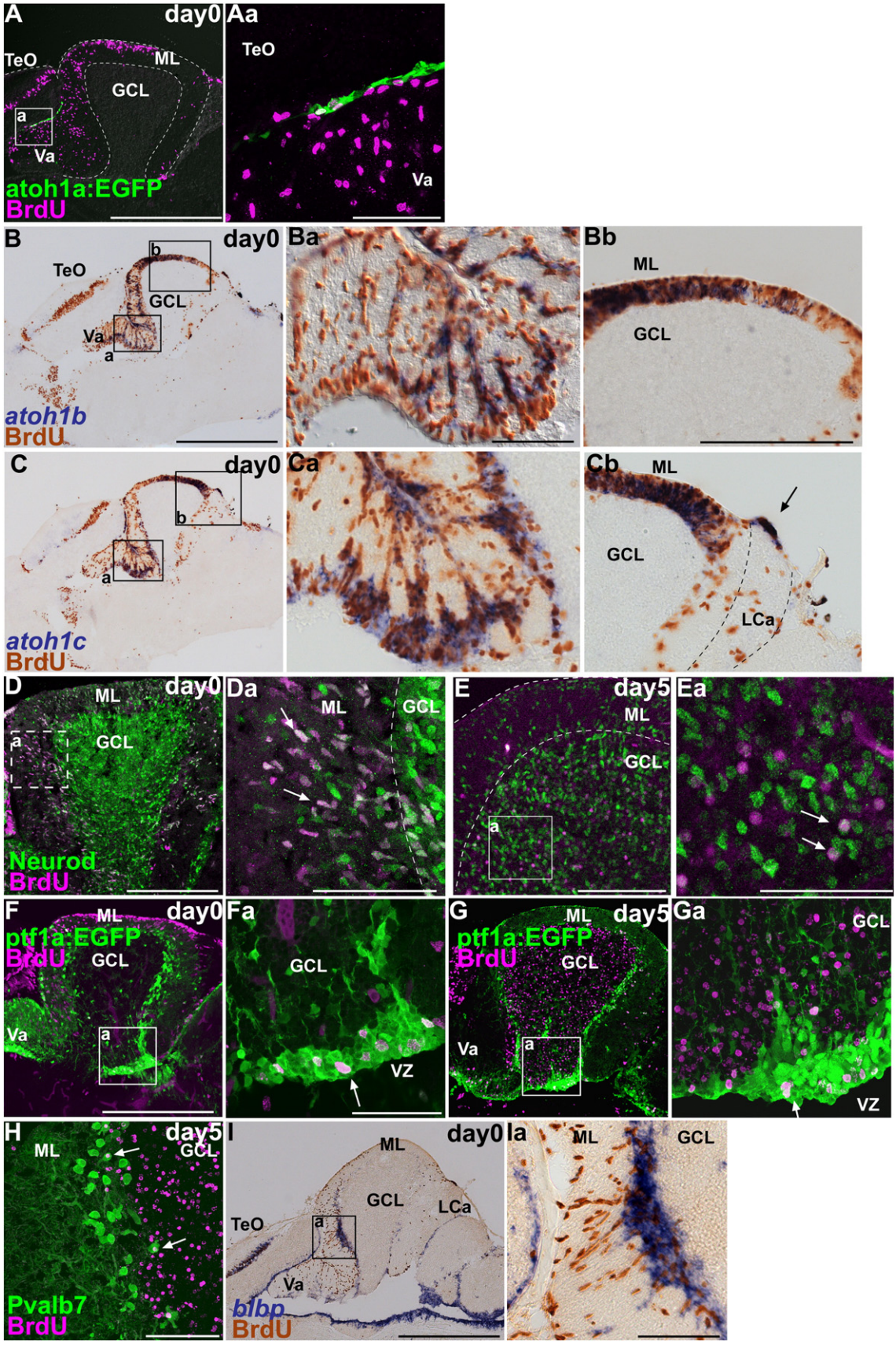
A
day0
TeO
ML
GCL
a
Va
atoh1a:EGFP
BrdU
Aa
TeO
Va
B
day0
b
TeO
GCL
Va
a
atoh1b
BrdU
Ba
Bb
ML
GCL
C
day0
b
a
atoh1c
BrdU
Ca
Cb
ML
GCL
LCa
D
day0
ML
a
GCL
Neurod
BrdU
Da
ML
GCL
E
day5
ML
GCL
a
Ea
F
day0
ML
ptf1a:EGFP
BrdU
GCL
Va
a
Fa
GCL
VZ
G
day5
ML
ptf1a:EGFP
BrdU
GCL
Va
a
Ga
GCL
VZ
H
day5
ML
GCL
Pvalb7
BrdU
I
day0
ML
GCL
LCa
TeO
a
Va
blbp
BrdU
Ia
ML
GCL

(Fig. 5A, D). The *atoh1a*$^+$ and *ptf1a*$^+$ lineages occupied the rostral and caudal halves of the cerebellum by 3 dpf (Fig. 5B, E). Migration of the two lineages in opposite directions further leads to the formation of cerebellar layers at 5 dpf (Fig. 5 C, F, I, J). During these periods, there was very low expression, if any, of Blbp in the cerebellar domain (data not shown). Therefore, the migration of the granule and Purkinje cells (and possibly of other interneurons) does not depend on Bergmann glia. This is in contrast to the migration of granule cells at the late larval and adult stages, which is believed to be guided by glial fibers (Kaslin et al., 2009; Rieger et al., 2009). Thus, the migration of the granule cells and GABAergic neurons may be regulated by different mechanisms at the early larval stage and the late larval and adult stages.

It is reported that the radial migration of the granule cells involves the Sema6–PlexinA2 system and N-cadherin (Cdh2), respectively, in the mouse (Kerjan et al., 2005; Renaud et al., 2008) and zebrafish (Rieger et al., 2009) cerebellum. However, it is not yet clear how the migration of the GABAergic neuron is controlled, and further studies are required to resolve this issue. The close contact between cells of the *atoh1a*$^+$ and *ptf1a*$^+$ lineages suggests that functional interactions between them are likely. In the mammalian cerebellum, Purkinje cells are thought to provide trophic support for granule cells (Smeyne et al., 1995; Wetts and Herrup, 1983). Purkinje cells express Sonic hedgehog (Shh) and promote the expansion of the granule cells (Dahmane and Ruiz i Altaba, 1999; Wallace, 1999; Wechsler-Reya and Scott, 1999). Although the role of Hh signaling in the early specification of granule cells in zebrafish is ambiguous (Chaplin et al., 2010), we have preliminary data from zebrafish in which the *ptf1a*$^+$ lineage is ablated that suggest that the generation of the Neurod$^+$ granule cells depends on the presence of the *ptf1a*$^+$ lineage (data not shown). Interactions between the two lineages (possibly Hh-independent signals) may therefore be important not only for the proliferation but also for the specification and migration of the granule cells and GABAergic neurons.

Origin of olig2$^+$ *eurydendroid cells*

Eurydendroid cells are the cerebellar projection neurons that transmit information from Purkinje cells to extracerebellar domains. Although the function of eurydendroid cells is equivalent to that of the neurons in the deep cerebellar nuclei of the mammalian cerebellum, whether the origins of these cell populations are similar is not known. The glutamatergic and GABAergic neurons in the deep cerebellar nuclei originate from the *Atoh1a*$^+$ URL and *Ptf1a*$^+$ VZ progenitors, respectively (Hoshino et al., 2005; Machold and Fishell, 2005; Wang et al., 2005). We previously reported the presence of two kinds of eurydendroid cells, the calretinin-immunoreactive (CR-ir$^+$) and the CR-ir$^-$, *olig2*$^+$ neurons, in the adult cerebellum (Bae et al., 2009). Here, we showed that the majority of *olig2*$^+$ eurydendroid cells are derived from the *ptf1a*$^+$ VZ progenitors and that some *olig2*$^+$ eurydendroid cells are derived from the *atoh1a*$^+$ URL progenitors, at the early larval stages (Fig. 6K–R).

The olig2:EGFP signals were detected in part of the domain populated by *ptf1a*$^+$ or *atoh1a*$^+$ progenitors (Fig. 6K–R), suggesting that the *olig2*$^+$ eurydendroid cells are derived from restricted areas in the URL and VZ. Although the *Ptf1a*$^+$ VZ progenitors generate only GABAergic neurons in the mouse deep cerebellar nuclei, the *olig2*$^+$ eurydendroid cells from both the *ptf1a*$^+$ VZ and *atoh1a*$^+$ URL progenitors were glutamatergic, suggesting that the development of the *olig2*$^+$ eurydendroid cells is different from that of the deep cerebellar nucleus neurons. Although the *Ptf1a*$^+$ VZ progenitors produce GABAergic neurons in the mammalian cerebellum, the hindbrain cochlear nucleus, the spinal cord, and the retina (Dullin et al., 2007; Fujiyama et al., 2009; Glasgow et al., 2005; Hoshino, 2006; Hoshino et al., 2005), they also produce glutamatergic neurons in the inferior olive nuclei of the hindbrain (Yamada et al., 2007). Therefore, the generation of glutamatergic neurons from *ptf1a*$^+$ progenitors is not unique to the central nervous system of teleost species. Studies of *Olig2*-expressing neurons and/or neuronal progenitors in the mouse cerebellum could provide a clue for understanding the evolution of cerebellar projection neurons.

As reported previously (McFarland et al., 2008), we found that a portion of Cr-ir$^+$ neurons were also olig2:EGFP$^+$, but the majority were olig2:EGFP$^-$ at the larval stage (data not shown). Cell tracing with permanent labeling (e.g. Cre-loxP mediated tracing) should reveal the origin of Cr-ir$^+$ eurydendroid cells.

Adult neurogenesis

Analyses of BrdU pulse-chase labeling and proliferation markers has shown that neural stem cells reside in the medial part of the molecular layer of the Va and CCe of the adult zebrafish cerebellum; their progeny differentiate into granule cells and migrate into the granule cell layer within a week (Kaslin et al., 2009; Zupanc et al., 2005). These proliferating cells are reported to express the neural stem cell markers Nestin, Sox2, and Musashi, but not the proneural genes *atoh1a*, *atoh1b,* or *ptf1a*; the Blbp$^+$ or S100β$^+$ glial cells do not proliferating, but they are associated with the neural stem cells (Kaslin et al., 2009). In contrast to this report, we detected the expression *atoh1a*, *atoh1b* and *atoh1c* in the molecular layer, and that of *ptf1a* in the VZ, of the adult cerebellum (Fig. 7), and we confirmed the expression of *atoh1a* and *ptf1a* by using the *Tg(atoh1a:EGFP)* and *Tg(ptf1a:EGFP)* lines (Fig. 8). Our data indicate that most if not all *atoh1a, atoh1b*, and/or *atoh1c*-expressing cells and some of the *ptf1a*-expressing cells are proliferating cells in the adult cerebellum (Fig. 8).

We also found that *blbp*-expressing cells could incorporate BrdU, and thus at least some Bergman glial cells are proliferating cells in the adult (Fig. 8I). This discrepancy may be attributable to the relatively low levels of proneural gene expression, and the difficulty of detecting the glial cell structure by immunostaining with the anti-Blbp antibodies. Our findings suggest that there are at least three distinct progenitor populations in the zebrafish adult cerebellum: *atoh1*$^+$ granule cell progenitors, *ptf1a*$^+$ GABAergic neuronal progenitors, and *blbp*$^+$ radial glial cells (Bergmann glial cells). Since the *atoh1*$^+$ URL and *ptf1a*$^+$ VZ progenitors generate, respectively, the granule cells and GABAergic neurons in the larval cerebellum, the same genetic cascades are likely to continuously provide cerebellar neurons in the adult. Considering the function of proneural genes, these proneural gene-expressing cells are probably committed to be either glutamatergic or GABAergic neurons. We hypothesize that the *atoh1*$^+$ or *ptf1a*$^+$ cells in adults do not generate

Fig. 8. Expression of proneural genes associates with cell proliferation in the adult cerebellum. (A–D) BrdU incorporation in *atoh1a, atoh1b, atoh1c,* or Neurod-expressing cells. Adult (about 3 months old) *Tg(atoh1a:EGFP)* or wild-type fish were labeled with BrdU for 1 h, and proliferating cells were analyzed by immunostaining with anti-BrdU antibody (magenta in A; brown in B and C), and anti-EGFP (green, A), anti-Neurod (green, D) antibodies, or *atoh1b* (purple, B) or *atoh1c* (purple, C) probes. Parasagittal (A) and sagittal sections near the midline (B–D). (Aa, Ba, Bb, Ca, Cb, and Da) High-magnification views of the boxes in (A–D). (E) Birthdate analysis of granule cells. Adult fish were labeled with BrdU and fixed 5 days after labeling (day 5). The cerebellum was stained with anti-BrdU (magenta) and Neurod (green) antibodies. Sagittal section. (Ea) High-magnification view of the box in (E). BrdU$^+$, Neurod$^+$ granule cells were detected in the molecular layer 1 h after labeling (arrows, Da), but were in the GCL at day 5 (arrows, Ea). (F) BrdU incorporation in *ptf1a*-expressing cells. Sagittal section (F) and high magnification view (Fa). BrdU$^+$, ptf1a:EGFP$^+$ cells were detected in the VZ (arrow). (G, H) Birthdate analyses of GABAergic lineage. Adult *Tg(ptf1a:EGFP)* (G) or wild-type (H) fish were labeled with BrdU, and the cerebellum was stained with anti-EGFP (G) or anti-Pvalb7 (H) antibodies on day 5. Sagittal sections (G, H) and high-magnification view (Ga). Many of the BrdU-positive cells stayed in the VZ (arrow, Ga), but BrdU$^+$, Pvalb7$^+$ Purkinje cells were detected (arrows, H) on day 5. (I) BrdU incorporation in *blbp*-expressing Bergmann glia. Sagittal section through the Va and the rostral CCe (I) and high-magnification view (Ia). Note that *blbp* signals overlap with the BrdU signals. The abbreviations are defined in Figs. 1 and 3. Scale bars: 50 μm (Aa, Ea), 100 μm (Ba, Da, E, Ia), 200 μm (D, Fa, H), 500 μm (A, Ba, F), 1 mm (B, I).

both neurons and glial (neural stem cells), but rather serve as neuronal progenitors that give rise only to neurons.

Blbp$^+$ GFAP$^+$ radial glial cells serve as neural precursors in the mammalian central nervous system (Hartfuss et al., 2001; Malatesta et al., 2003, 2000; Pinto and Gotz, 2007; Ponti et al., 2008). Our data suggest that Bergmann glial cells, which express Blbp but not GFAP in the adult cerebellum of the zebrafish (Bae et al., 2009), also function as neural precursors. It is not clear whether Bergmann glial cells generate both neurons and glia. Birthdate analysis revealed that S100β$^+$ glial cells are generated in the adult cerebellum (Kaslin et al., 2009; Zupanc et al., 2005). It is possible that Bergmann glial cells, which are negative for S100β, generate the S100β$^+$ glial cells. Alternatively, like the radial glia of the mammalian central nervous system, Bergmann glia may serve as true neural stem cells in the adult cerebellum, producing both glia and neuronal progenitors (e.g. *atoh1*$^+$ progenitors) that give rise to cerebellar neurons (granule cells). Lineage tracing of Bergmann glial cells and the *atoh1*$^+$ and *ptf1a*$^+$ progenitors, should clarify the fate of these three progenitor populations, and the relationship between these progenitors and the Nestin$^+$, Sox2$^+$, and Musashi$^+$ neural stem cells reported previously (Kaslin et al., 2009).

As in the larval stages, we found that Neurod$^+$ immature granule cells in the molecular layer of the adult cerebellum proliferated and migrated rapidly inward, to the granule cell layer (Fig. 8D, E). These data further indicate that the expansion and migration of the granule cells in the adult is essentially an extension of larval neurogenesis. In contrast to the granule cell progenitors, only a portion of the ptf1a: EGFP$^+$ cells were proliferating (Fig. 8G), and a small population of BrdU$^+$ Purkinje cells was detected 5 days after labeling (Fig. 8H), suggesting that the turnover of the Purkinje cells and other GABAergic neurons in the adult zebrafish cerebellum is very slow. These data suggest that the granule cells, which relay mossy fiber information, play more important roles than Purkinje cells in remodeling cerebellar neural circuits for the higher motor control and learning behaviors of adult fish. Selected inhibition of adult neurogenesis using the regulatory elements of the proneural genes and the glial gene will reveal the role of adult neurogenesis in zebrafish. Therefore, the zebrafish cerebellum provides a model for studying neurogenesis and remodeling of the neural circuits in vertebrate brains.

Acknowledgments

We thank B. Appel for the *Tg(olig2:EGFP)vu12* line; S.D. Leach for the *Tg(ptf1a:EGFP)jh1* line; H. Baier for comments on the manuscript; K. Bando, S. Fujii, and A. Katsuyama for technical assistance; and the members of the Hibi Laboratory for helpful discussions. This work was supported by a grant from NCC, Korea (NCC-1010270 to Y.-K., B.) and by a grant from RIKEN (to M.H.).

Appendix A. Supplementary data

Supplementary data associated with this article can be found, in the online version, at doi:10.1016/j.ydbio.2010.03.024.

References

Adolf, B., Bellipanni, G., Huber, V., Bally-Cuif, L., 2004. atoh1.2 and beta3.1 are two new bHLH-encoding genes expressed in selective precursor cells of the zebrafish anterior hindbrain. Gene Expr. Patterns 5, 35–41.

Adolf, B., Chapouton, P., Lam, C.S., Topp, S., Tannhauser, B., Strahle, U., Gotz, M., Bally-Cuif, L., 2006. Conserved and acquired features of adult neurogenesis in the zebrafish telencephalon. Dev. Biol. 295, 278–293.

Alder, J., Cho, N.K., Hatten, M.E., 1996. Embryonic precursor cells from the rhombic lip are specified to a cerebellar granule neuron identity. Neuron 17, 389–399.

Altman, J., 1969. Autoradiographic and histological studies of postnatal neurogenesis. IV. Cell proliferation and migration in the anterior forebrain, with special reference to persisting neurogenesis in the olfactory bulb. J. Comp. Neurol. 137, 433–457.

Altman, J., Bayer, S.A., 1997. Developmentof the cerebellar system in relation to its evolution, structure, and function. CRC Press, Inc., Boca Raton, FL.

Altman, J., Das, G.D., 1965. Autoradiographic and histological evidence of postnatal hippocampal neurogenesis in rats. J. Comp. Neurol. 124, 319–335.

Alvarez Otero, R., Sotelo, C., Alvarado-Mallart, R.M., 1993. Chick/quail chimeras with partial cerebellar grafts: an analysis of the origin and migration of cerebellar cells. J. Comp. Neurol. 333, 597–615.

Bae, Y.K., Shimizu, T., Hibi, M., 2005. Patterning of proneuronal and inter-proneuronal domains by hairy- and enhancer of split-related genes in zebrafish neuroectoderm. Development 132, 1375–1385.

Bae, Y.K., Kani, S., Shimizu, T., Tanabe, K., Nojima, H., Kimura, Y., Higashijima, S., Hibi, M., 2009. Anatomy of zebrafish cerebellum and screen for mutations affecting its development. Dev. Biol. 330, 406–426.

Balaban, C.D., McGee, D.M., Zhou, J., Scudder, C.A., 2002. Responses of primate caudal parabrachial nucleus and Kolliker-fuse nucleus neurons to whole body rotation. J. Neurophysiol. 88, 3175–3193.

Ben-Arie, N., Bellen, H.J., Armstrong, D.L., McCall, A.E., Gordadze, P.R., Guo, Q., Matzuk, M.M., Zoghbi, H.Y., 1997. Math1 is essential for genesis of cerebellar granule neurons. Nature 390, 169–172.

Butler, A.B., Hodos, H., 1996. Comparative vertebrate neuroanatomy: evolution and adaptation. Wiley-Liss, New York.

Chaplin, N., Tendeng, C., Wingate, R.J., 2010. Absence of an external germinal layer in zebrafish and shark reveals a distinct, anamniote ground plan of cerebellum development. J. Neurosci. 30, 3048–3057.

Dahmane, N., Ruiz i Altaba, A., 1999. Sonic hedgehog regulates the growth and patterning of the cerebellum. Development 126, 3089–3100.

Davison, J.M., Akitake, C.M., Goll, M.G., Rhee, J.M., Gosse, N., Baier, H., Halpern, M.E., Leach, S.D., Parsons, M.J., 2007. Transactivation from Gal4-VP16 transgenic insertions for tissue-specific cell labeling and ablation in zebrafish. Dev. Biol. 304, 811–824.

Dullin, J.P., Locker, M., Robach, M., Henningfeld, K.A., Parain, K., Afelik, S., Pieler, T., Perron, M., 2007. Ptf1a triggers GABAergic neuronal cell fates in the retina. BMC Dev. Biol. 7, 110.

Ekström, P., Johnsson, C.M., Ohlin, L.M., 2001. Ventricular proliferation zones in the brain of an adult teleost fish and their relation to neuromeres and migration (secondary matrix) zones. J. Comp. Neurol. 436, 92–110.

Elsen, G.E., Choi, L.Y., Prince, V.E., Ho, R.K., 2009. The autism susceptibility gene met regulates zebrafish cerebellar development and facial motor neuron migration. Dev. Biol. 335, 78–92.

Eriksson, P.S., Perfilieva, E., Bjork-Eriksson, T., Alborn, A.M., Nordborg, C., Peterson, D.A., Gage, F.H., 1998. Neurogenesis in the adult human hippocampus. Nat. Med. 4, 1313–1317.

Fujiyama, T., Yamada, M., Terao, M., Terashima, T., Hioki, H., Inoue, Y.U., Inoue, T., Masuyama, N., Obata, K., Yanagawa, Y., Kawaguchi, Y., Nabeshima, Y., Hoshino, M., 2009. Inhibitory and excitatory subtypes of cochlear nucleus neurons are defined by distinct bHLH transcription factors, Ptf1a and Atoh1. Development 136, 2049–2058.

Glasgow, S.M., Henke, R.M., Macdonald, R.J., Wright, C.V., Johnson, J.E., 2005. Ptf1a determines GABAergic over glutamatergic neuronal cell fate in the spinal cord dorsal horn. Development 132, 5461–5469.

Gould, E., Tanapat, P., McEwen, B.S., Flugge, G., Fuchs, E., 1998. Proliferation of granule cell precursors in the dentate gyrus of adult monkeys is diminished by stress. Proc. Natl. Acad. Sci. U. S. A. 95, 3168–3171.

Grandel, H., Kaslin, J., Ganz, J., Wenzel, I., Brand, M., 2006. Neural stem cells and neurogenesis in the adult zebrafish brain: origin, proliferation dynamics, migration and cell fate. Dev. Biol. 295, 263–277.

Hallonet, M.E., Teillet, M.A., Le Douarin, N.M., 1990. A new approach to the development of the cerebellum provided by the quail-chick marker system. Development 108, 19–31.

Hartfuss, E., Galli, R., Heins, N., Gotz, M., 2001. Characterization of CNS precursor subtypes and radial glia. Dev. Biol. 229, 15–30.

Hashimoto, M., Mikoshiba, K., 2003. Mediolateral compartmentalization of the cerebellum is determined on the "birth date" of Purkinje cells. J. Neurosci. 23, 11342–11351.

Hoshino, M., 2006. Molecular machinery governing GABAergic neuron specification in the cerebellum. Cerebellum 5, 193–198.

Hoshino, M., Nakamura, S., Mori, K., Kawauchi, T., Terao, M., Nishimura, Y.V., Fukuda, A., Fuse, T., Matsuo, N., Sone, M., Watanabe, M., Bito, H., Terashima, T., Wright, C.V., Kawaguchi, Y., Nakao, K., Nabeshima, Y., 2005. Ptf1a, a bHLH transcriptional gene, defines GABAergic neuronal fates in cerebellum. Neuron 47, 201–213.

Ito, M., 2002a. Historical review of the significance of the cerebellum and the role of Purkinje cells in motor learning. Ann. N. Y. Acad. Sci. 978, 273–288.

Ito, M., 2002b. The molecular organization of cerebellar long-term depression. Nat. Rev. Neurosci. 3, 896–902.

Ito, M., 2006. Cerebellar circuitry as a neuronal machine. Prog. Neurobiol. 78, 272–303.

Ito, M., 2008. Control of mental activities by internal models in the cerebellum. Nat. Rev. Neurosci. 9, 304–313.

Kaslin, J., Ganz, J., Geffarth, M., Grandel, H., Hans, S., Brand, M., 2009. Stem cells in the adult zebrafish cerebellum: initiation and maintenance of a novel stem cell niche. J. Neurosci. 29, 6142–6153.

Kerjan, G., Dolan, J., Haumaitre, C., Schneider-Maunoury, S., Fujisawa, H., Mitchell, K.J., Chedotal, A., 2005. The transmembrane semaphorin Sema6A controls cerebellar granule cell migration. Nat. Neurosci. 8, 1516–1524.

Kim, C.H., Bae, Y.K., Yamanaka, Y., Yamashita, S., Shimizu, T., Fujii, R., Park, H.C., Yeo, S.Y., Huh, T.L., Hibi, M., Hirano, T., 1997. Overexpression of neurogenin induces ectopic expression of HuC in zebrafish. Neurosci. Lett. 239, 113–116.

Kimura, Y., Okamura, Y., Higashijima, S., 2006. alx, a zebrafish homolog of Chx10, marks ipsilateral descending excitatory interneurons that participate in the regulation of spinal locomotor circuits. J. Neurosci. 26, 5684–5697.

Köster, R.W., Fraser, S.E., 2001. Direct imaging of in vivo neuronal migration in the developing cerebellum. Curr. Biol. 11, 1858–1863.

Köster, R.W., Fraser, S.E., 2006. FGF signaling mediates regeneration of the differentiating cerebellum through repatterning of the anterior hindbrain and reinitiation of neuronal migration. J. Neurosci. 26, 7293–7304.
Lee, E.C., Yu, D., Martinez de Velasco, J., Tessarollo, L., Swing, D.A., Court, D.L., Jenkins, N.A., Copeland, N.G., 2001. A highly efficient *Escherichia coli*-based chromosome engineering system adapted for recombinogenic targeting and subcloning of BAC DNA. Genomics 73, 56–65.
Lin, J.W., Biankin, A.V., Horb, M.E., Ghosh, B., Prasad, N.B., Yee, N.S., Pack, M.A., Leach, S.D., 2004. Differential requirement for ptf1a in endocrine and exocrine lineages of developing zebrafish pancreas. Dev. Biol. 270, 474–486.
Lois, C., Alvarez-Buylla, A., 1994. Long-distance neuronal migration in the adult mammalian brain. Science 264, 1145–1148.
Luskin, M.B., 1993. Restricted proliferation and migration of postnatally generated neurons derived from the forebrain subventricular zone. Neuron 11, 173–189.
Machold, R., Fishell, G., 2005. Math1 is expressed in temporally discrete pools of cerebellar rhombic-lip neural progenitors. Neuron 48, 17–24.
Malatesta, P., Hartfuss, E., Gotz, M., 2000. Isolation of radial glial cells by fluorescent-activated cell sorting reveals a neuronal lineage. Development 127, 5253–5263.
Malatesta, P., Hack, M.A., Hartfuss, E., Kettenmann, H., Klinkert, W., Kirchhoff, F., Gotz, M., 2003. Neuronal or glial progeny: regional differences in radial glia fate. Neuron 37, 751–764.
Mathis, L., Nicolas, J.F., 2003. Progressive restriction of cell fates in relation to neuroepithelial cell mingling in the mouse cerebellum. Dev. Biol. 258, 20–31.
Mathis, L., Bonnerot, C., Puelles, L., Nicolas, J.F., 1997. Retrospective clonal analysis of the cerebellum using genetic laacZ/lacZ mouse mosaics. Development 124, 4089–4104.
McFarland, K.A., Topczewska, J.M., Weidinger, G., Dorsky, R.I., Appel, B., 2008. Hh and Wnt signaling regulate formation of olig2+ neurons in the zebrafish cerebellum. Dev. Biol. 318, 162–171.
Miyamura, Y., Nakayasu, H., 2001. Zonal distribution of Purkinje cells in the zebrafish cerebellum: analysis by means of a specific monoclonal antibody. Cell Tissue Res. 305, 299–305.
Miyata, T., Maeda, T., Lee, J.E., 1999. NeuroD is required for differentiation of the granule cells in the cerebellum and hippocampus. Genes Dev. 13, 1647–1652.
Mueller, T., Wullimann, M.F., 2002. BrdU-, neuroD (nrd)- and Hu-studies reveal unusual non-ventricular neurogenesis in the postembryonic zebrafish forebrain. Mech. Dev. 117, 123–135.
Pinto, L., Gotz, M., 2007. Radial glial cell heterogeneity–the source of diverse progeny in the CNS. Prog. Neurobiol. 83, 2–23.
Pisharath, H., Rhee, J.M., Swanson, M.A., Leach, S.D., Parsons, M.J., 2007. Targeted ablation of beta cells in the embryonic zebrafish pancreas using *E. coli* nitroreductase. Mech. Dev. 124, 218–229.
Ponti, G., Peretto, P., Bonfanti, L., 2008. Genesis of neuronal and glial progenitors in the cerebellar cortex of peripuberal and adult rabbits. PLoS ONE 3, e2366.
Renaud, J., Kerjan, G., Sumita, I., Zagar, Y., Georget, V., Kim, D., Fouquet, C., Suda, K., Sanbo, M., Suto, F., Ackerman, S.L., Mitchell, K.J., Fujisawa, H., Chedotal, A., 2008. Plexin-A2 and its ligand, Sema6A, control nucleus-centrosome coupling in migrating granule cells. Nat. Neurosci. 11, 440–449.
Rieger, S., Senghaas, N., Walch, A., Köster, R.W., 2009. Cadherin-2 controls directional chain migration of cerebellar granule neurons. PLoS Biol. 7, e1000240.
Scott, E.K., Baier, H., 2009. The cellular architecture of the larval zebrafish tectum, as revealed by gal4 enhancer trap lines. Front. Neural Circuits 3, 13.
Scott, E.K., Mason, L., Arrenberg, A.B., Ziv, L., Gosse, N.J., Xiao, T., Chi, N.C., Asakawa, K., Kawakami, K., Baier, H., 2007. Targeting neural circuitry in zebrafish using GAL4 enhancer trapping. Nat. Methods 4, 323–326.
Shin, J., Park, H.C., Topczewska, J.M., Mawdsley, D.J., Appel, B., 2003. Neural cell fate analysis in zebrafish using olig2 BAC transgenics. Methods Cell Sci. 25, 7–14.
Smeyne, R.J., Chu, T., Lewin, A., Bian, F., Sanlioglu, S., Kunsch, C., Lira, S.A., Oberdick, J., 1995. Local control of granule cell generation by cerebellar Purkinje cells. Mol. Cell. Neurosci. 230–251.
Thisse, C., Thisse, B., 1998. High resolution whole-mount in situ hybridization. Zebrafish Science Monitor.
Volkmann, K., Rieger, S., Babaryka, A., Köster, R.W., 2008. The zebrafish cerebellar rhombic lip is spatially patterned in producing granule cell populations of different functional compartments. Dev. Biol. 313, 167–180.
Wallace, V.A., 1999. Purkinje-cell-derived Sonic hedgehog regulates granule neuron precursor cell proliferation in the developing mouse cerebellum. Curr. Biol. 9, 445–448.
Wang, V.Y., Rose, M.F., Zoghbi, H.Y., 2005. Math1 expression redefines the rhombic lip derivatives and reveals novel lineages within the brainstem and cerebellum. Neuron 48, 31–43.
Wang, Y., Chen, K., Yao, Q., Zheng, X., Yang, Z., 2009. Phylogenetic analysis of zebrafish basic helix–loop–helix transcription factors. J. Mol. Evol. 68, 629–640.
Wechsler-Reya, R.J., Scott, M.P., 1999. Control of neuronal precursor proliferation in the cerebellum by Sonic Hedgehog. Neuron 22, 103–114.
Westerfield, M., 1995. The zebrafish book. The University of Oregon Press.
Wetts, R., Herrup, K., 1983. Direct correlation between Purkinje and granule cell number in the cerebella of lurcher chimeras and wild-type mice. Brain Res. 312, 41–47.
Wilson, L.J., Wingate, R.J., 2006. Temporal identity transition in the avian cerebellar rhombic lip. Dev. Biol. 297, 508–521.
Wingate, R.J., 2001. The rhombic lip and early cerebellar development. Curr. Opin. Neurobiol. 11, 82–88.
Wingate, R., 2005. Math-Map(ic)s. Neuron 48, 1–4.
Wullimann, M.F., Knipp, S., 2000. Proliferation pattern changes in the zebrafish brain from embryonic through early postembryonic stages. Anat. Embryol. (Berl.) 202, 385–400.
Wullimann, M.F., Mueller, T., 2002. Expression of Zash-1a in the postembryonic zebrafish brain allows comparison to mouse Mash1 domains. Brain Res. Gene Expr. Patterns 1, 187–192.
Wullimann, M.F., Rupp, B., Reichert, H., 1996. Neuroanatomy of the zebrafish brain: a topological atlas. Birkhäuser Verlag, Basel.
Yamada, M., Terao, M., Terashima, T., Fujiyama, T., Kawaguchi, Y., Nabeshima, Y., Hoshino, M., 2007. Origin of climbing fiber neurons and their developmental dependence on Ptf1a. J. Neurosci. 27, 10924–10934.
Yeomans, J.S., 1995. Role of tegmental cholinergic neurons in dopaminergic activation, antimuscarinic psychosis and schizophrenia. Neuropsychopharmacology 12, 3–16.
Zecchin, E., Mavropoulos, A., Devos, N., Filippi, A., Tiso, N., Meyer, D., Peers, B., Bortolussi, M., Argenton, F., 2004. Evolutionary conserved role of ptf1a in the specification of exocrine pancreatic fates. Dev. Biol. 268, 174–184.
Zhang, L., Goldman, J.E., 1996. Generation of cerebellar interneurons from dividing progenitors in white matter. Neuron 16, 47–54.
Zikopoulos, B., Kentouri, M., Dermon, C.R., 2000. Proliferation zones in the adult brain of a sequential hermaphrodite teleost species (Sparus aurata). Brain Behav. Evol. 56, 310–322.
Zupanc, G.K., Horschke, I., 1995. Proliferation zones in the brain of adult gymnotiform fish: a quantitative mapping study. J. Comp. Neurol. 353, 213–233.
Zupanc, G.K., Hinsch, K., Gage, F.H., 2005. Proliferation, migration, neuronal differentiation, and long-term survival of new cells in the adult zebrafish brain. J. Comp. Neurol. 488, 290–319.